Publicaciones
Geológicas
Especiales
Del
Ingeominas

ISSN - 0120 - 078X

THE ANTIOQUIAN BATHOLITH, COLOMBIA

By

TOMAS FEININGER
Escuela Politécnica Nacional
Quito, Ecuador

and

GERARDO BOTERO A.
Medellín, Colombia

No. 12, pp. 1 - 50, 1982
Bogotá - Colombia
ISSN - 0120 - 078X

Pub. Geol. Esp.

REPUBLICA DE COLOMBIA

MINISTERIO DE MINAS Y ENERGIA
Carlos Martínez Simahan, Ministro

INSTITUTO NACIONAL DE INVESTIGACIONES GEOLOGICO - MINERAS
Alfonso López Reina, Director General

THE ANTIOQUIAN BATHOLITH, COLOMBIA

By

TOMAS FEININGER
Escuela Politécnica Nacional
Quito, Ecuador[1]

and

GERARDO BOTERO A.
Medellín, Colombia

1) Present address: Département de Geologie, Université Laval, Québec, Qué. Canádá GIK 7P4

No. 12, pp. 1 - 50, 1982
Bogotá - Colombia
ISSN - 0120 - 078X

Pub. Geol. Esp.
Ingeominas

INGEOMINAS: Instituto Nacional de Investigaciones Geológico - Mineras
Diag. 53 No. 34 - 53, Apartado Aéreo No. 4865
Bogotá 2, D.E., Colombia, S. A.

Publicación no periódica
Formato de publicación: 17 x 24 cm

Editor:

ALBERTO VILLEGAS BETANCOURT

Geólogo

Precio de cada ejemplar:	Ingeominas	$ 200.00	(US $5.00)
	Vía Aérea	$ 250.00	(US $6.50)

Editado e impreso por Ingeominas

CONTENIDO

FIGURES

TABLES

ABSTRACT

The Antioquian batholith has an exposed area of 7221 km^2 in the Central Andean Cordillera of Colombia. The batholith is monotonously uniform; 97 percent is quartz diorite or granodiorite composed of quartz (23.9 per cent, average), K feldspar (6.7), plagioclase (48.4; $An_{43.5}$), hornblende (9.3), biotite (9.3) secondary chlorite (1.6), and accesory minerals (0.8). Minor felsic and gabbroic facies have been recognized locally. Numerous broadly concordant radiometric ages show the batholith to be Late Cretaceous. Andesite dikes, mostly between 2 cm and 1 m thick, are common throughout the batholith. Felsic dikes are rare.

Longitudinal variations of modal composition and petrographic characteristics are present. From east to west, the batholith is progressively poorer in K feldspar, has a higher color index and increasingly shows effects of postintrusive deformation.

Batholith rock is mostly massive. Mafic clots ("gabarros") are common features, and typically display little or no preferred orientation. The contact of the batholith with regionally metamorphic hostrocks is discordant and sharp, except against amphibolite where mixing has taken place. The roof of the batholith appears to be a nearly planar surface, broken in places by regional "intrusion faults". The roof increases in elevation progressively from east to west at from 20 to 30 m/km. Postemplacement faults and regional shear zones cut the batholith in places.

The following observations attest to the emplacement of the Antioquian batholith by the intrusion of hot, fluid, uniform magma: sharp and discordant contacts, rotated inclusions, discordant apophyses in hostrocks, modal homogeneity, hypidiomorphic equigranular igneous texture, and an enclosing high-temperature thermal aureole. The magma may have been derived by the partial fusion of deep rocks in a relatively dry environment. The Antioquian batholith is interpreted to have the form of an enormous subhorizontal intrusive sheet or dike with little thickness relative to its exposed breadth. Lateral intrusion of magma may have lifted the roof of the batholith as a nearly integral unit. Sheetlike intrusions with forms similar to thar postulated for the Antioquian batholith have been described in Colorado (USA) and Antarctica.

RESUMEN

El batolito antioqueño aflora en un área de 7221 km^2, localizada en la Cordillera Central de Colombia. El batolito es de una uniformidad monótona; 97% es cuarzodiorita o granodiorita, compuesta de cuarzo (23.9% en promedio), feldespato de potasio (6.7%), plagioclasa (48.4%; $An_{43.5}$), hornblenda (9.3%), biotita (9.3%), clorita secundaria (1.6) y minerales accesorios (0.8%).

Facies menores félsicas y gabróideas se han reconocido localmente. Numerosas edades radiométricas, tolerablemente concordantes, indican que el batolito es de edad cretácea superior. Son comunes en el batolito diques andesíticos con espesores comprendidos entre 2 cm y 1 m. Los diques felsíticos son raros.

Se encuentran variaciones longitudinales en las composiciones modales y en las características petrográficas. De este a oeste el batolito es progresivamente más pobre en feldespato de potasio, muestra un índice de coloración más alto y la deformación post-intrusiva aumenta.

La roca del batolito es maciza en su mayoría. Una característica común la presentan las inclusiones máficas ("gabarros") que muestran muy poca o ninguna preferencia en su orientación. El contacto del batolito es discordante y neto con las rocas metamórficas encajantes, salvo con las anfibolitas donde ha habido mezcla. El techo del batolito parece ser una superficie casi plana interrumpida en algunos lugares por "fallas de intrusión". De este a oeste la elevación del techo aumenta progresivamente, de 20 a 30 m por km. Fallas postintrusivas y zonas de cizalladura regionales, cortan el batolito en algunos lugares.

El acomodamiento del batolito antioqueño por la intrusión de un magma fluido, caliente y uniforme, es atestiguado por las siguientes observaciones: contactos netos y discordantes, inclusiones desplazadas y rotadas, apófisis discordantes en las rocas encajantes, homogeneidad en la composición modal, textura ígnea hipidiomórfica equigranular y por último la existencia de una aureola envolvente de origen térmico y alta temperatura. El magma puede haberse originado por fusión parcial de rocas profundas en un medio relativamente seco. Se interpreta el Batolito Antioqueño como una gran intrusión en forma de manto subhorizontal y de espesor relativamente pequeño con relación al área expuesta. El techo del batolito puede haber sido levantado como una unidad integral, por la intrusión lateral del magma. Se han descrito intrusiones en forma de manto, como la propuesta para el Batolito Antioqueño, en Colorado (USA) y Antártica.

1. INTRODUCTION

Extensive parts of the eastern rim of the Pacific basin are bordered by inmense granitic batholiths. These batholiths are the dominant structural elements over much of the great cordilleras which run without interruption along the western borders of North and South America and through parts of Central America. The ages of the batholiths are predominantly Mesozoic and Cenozoic, although Paleozoic batholiths are important in Chile and Bolivia (RUIZ, and others,1961). In the past two decades, serveral detailed studios have been published on these batholiths in North America, particularly in California (BATEMAN, and others, 1963; BATEMAN and EATON, 1967; EVERNDEN and KISTLER, 1970; EVERNDEN and SHAW, 1971). The geology of the Central and South American batholiths is far less well known; indeed, only a few of these have been studied in detail (COBBING and PITCHER, 1972; MYERS, 1975), and no field studies have appeared in the more widely circulated geological literature.

The Antioquian batholith, with and area of 7221 km^2, is the largest and northernmost batholith of the Central Cordillera of the Colombian Andes. It is located in, and takes its name (BOTERO, 1940) from the Departamento (State) of Antioquia, whose capital, Mellín, lies inmediately west of the batholith.

With the current explosive growth of interest in the circum-Pacific area as a global geologic province, we feel that the results of recent mapping of the Antioquian batholith and our subsequent laboratory studies of selected rock samples may interest more than a local readership.

NOTE: Reasons beyond the control of the authors have delayed the publication of this paper, originally written in 1973. The extensive field and laboratory work reported herein, and the absence of any intervening report that focuses on this interesting and important pluton, constitute adequate justification for this late printing.

2. FIELD AND LABORATORY METHODS

The antioquian batholith, its contacts, and adjacent rocks were mapped at scale ranging from 1:100,000 to 1:25,000 between 1959 and 1968 by geologists of the Colombian Inventario Minero Nacional (now renamed INGEOMINAS), students and staff of the Facultad Nacional de Minas, Medellín, and ourselves (BOTERO A., 1963; INVENTARIO MINERO NACIONAL, 1965; ALVAREZ, J., HALL, R.B., and others, 1970; FEININGER, T., and others, 1970). Work was begun by Botero, A. and his students in the vicinity of Medellín. Subsequent mapping by Inventario geologists and Feininger in the northwest corner and east half of the batholith and adjacent areas was late in 1964 and largely completed within three years.

Most of the batholith is relatively easily accessible. It is crossed by the narrow-gauge Antioquian Railroad and few places are farther than 10 or 15 km from a road. Principal access, however, is by mule trail. A tigh network of literaly thousands of kilometers of such trails criss-cross the batholith.

From more than 1000 samples collected in the field, we selected 214 judged to be representative of the dominant normal facies of the batholith in their respective areas (an average of one sample every 32.7 km^2), and an additional 30 samples of minor facies and dikes. A standard thin section of each of these samples was studied and, excluding those cut from aphanitic or very fine-grained dikes, each was modally analyzed by either point-count (by Feininger) or Rosiwall (by Botero) methods. Most pointcount analyses are Rosiwall traverses excedd 50 cm. Staining of thind sections was not necessary as potassium feldspar and the dominant relatively calcic plagioclase are readily distinguished from one another and from quartz by their respective strong negative and positive relief. Identification of colored and accesorry minerals in the mostly unaltered rocks offered no difficulty. Rocks were named based on their modal composition following the classifiation proposed by O'Connor (1965).

We must here stress that our microscopic methods of modal analysis on the medium -to coarse- grained batholith rocks are not wholly satisfactory and should be considered only semi-quantitative. We tested the accuracy of our modal analysis by exchanging several thin sections between ourselves to repeat the other's analysis. In most cases the agreement was acceptable; generally, values fell within 10 percent of the value for each major mineral. Values for accesory minerals varied more widely. Nevertheless, even with these short comings in mind, our analysis are far superior to estimated modes, and the accuracy of the values given for the composition of the entire batholith obtained from the average of individual analysis is greatly enhanced by the large number of samples used.

Four samples of batholith rocks were chemically analyzed, and hornblendes in five samples of the normal facies were analyzed with the electron microprobe. Plagioclase compositions of all rocks were determined using flat stage techniques. Measurements were made on nonzoned or on the most weakly zoned grains found appropiatelly oriented in each thin section. The specific gravity of each unweathered sample was determined.

Samples 2 through 2687 are in the petrographic collection of the Facultad Nacional Nacional de Minas, Medellín, and samples 5043 through 8681 and JL-61, JL-63, and RAA-21 are in storage at INGEOMINAS, Medellín.

3. GEOGRAPHIC COORDINATES

Samples localities and critical exposures are cited using the Colombian national grid system. The grid is in meters and has the values X = 1.000.000 and Y = 1.000.000 m at the capital city Bogotá. Values increase northward and eastward, respectively. Thus Medellín, at X = 1.183.000 and Y = 835.350, lies on a parallel 183,00 km north of Bogotá and 164,65 km to the west. The third unit of the coordinate trinomial, Z, is the elevation in meters above sea level.

4. GEOMORPHOLOGY

4.1. CLIMATE

A humid tropical climate prevails over the Antioquian batholith and surrounding rocks. Diurnal average temperatures vary from place to place depending chiefly on elevation and to a lesser extent on topographic setting. The near equatorial location of the batholith precludes seasonal variations, and frosts are unknown even on the highest peaks, about 3100 m above sea level. Rainfall is not evenly distributed, but falls mostly in two wet season; April through June and September through November. Spells of more than a month without rain are unusual and the indigenoues forest as well as cleared pasture vegetation remain green throughout the year. Meteorologic data from eight stations on or near the Antioquian batholith are summarized in Table I.

TABLE 1.

METEOROLOGIC DATA FROM EIGHT STATION ON OR NEAR THE ANTIOQUIAN BATHOLITH[1]

Station	Coordinates X	Coordinates Y	Elevation (m)	Anual rainfall. (mm)	Temperature (°C) Min.	Temperature (°C) Max.	Temperature (°C) Ave.	Years Record
Barbosa	1,203,500	861,400	1,300	1,658	–	–	22	8
Cisneros	1,215,000	888,500	1,080	3,524	14,5	35,0	25	7
Medellín	1,183,000	835,350	1,538	1,413	10,0	31,6	21,4	60
Rionegro	1,172,400	856,500	2,120	1,977	7,0	27,2	18,4	10
San Luis	1,160,000	898,600	1,115	5,725	13,0	34,0	24,6	5
Santa Rosa	1,227,000	847,200	2,562	2,038	–	–	15	7
Segovia	1,274,800	931,500	650	2,891	–	–	24	8
Yarumal	1,261,600	852,000	2,300	3,706	8,4	26,5	17,3	6

1 Data mostly from Departamento de Planeación, Medellín.

4.2. WEATHERING

The generally hot climate and abundant rainfall promote intense chemical decomposition of the bedrock which in turn has produced a thick and nearly ubiquitous mantle of rotted rock. This mantle is thickest in areas of little local relief where erosion by running water and mass wasting are slight. For example, a series of 117 test borings located in different hydroelectric proyects on the Antioquian batholith (Troneras Proyect, 16 test borings; Punchiná (Samaná), 26 test borings; Las Playas, 40 test borings; Jaguas 33 test borings) shows the average depth to fresh rock to be 34,2 m and in places it is as much as 80 m (FEININGER, 1971; EMPRESAS PUBLICAS DE MEDELLIN, 1957, 1971) (Fig.1).

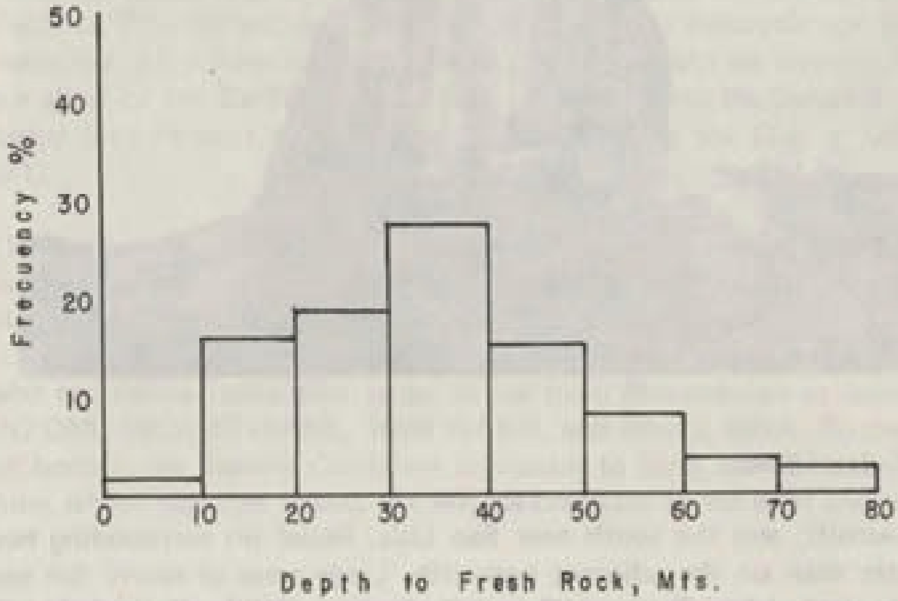

FIGURE 1. Depth of weathering on the Antioquian batholith as shown by 117 test borings at hydroelectric proyects at Troneras, Punchiná, Las Playas, and Jaguas.

Unlike the surrounding foliated and layered metamorphic and sedimentary rocks, the granitic rock of the Antioquian atholith is massive. Chemical decomposition does not pervasively attack this rock, but acts chiefly along joints and other fractures. As joints are relatively widely spaced over much of the batholith, decomposition of batholith rock in the rotted mantle is incomplete and the mantle generally contains an abundance of rounded residual boulders of fresh rock from one to 40 m in diameter. The rotted rock that surrounds these boulders is a relatively easily eroded so that with time the residual boulders become exposed.

A spotty carpet of these boulders is a conspicuous feature of much of the landscape underlain by the Antioquian batholith (FEININGER, 1969-1971; see also BRANNER,1896; WILHELMY, 1958). Where joints are exceptionally widely spaced, enormous monoliths of fresh rock are bared by the same mechanism. These monoliths in Antioquia have been named **peñoles** by Botero A. (1963, p. 28) and are probably rooted to fresh rock at depth. The largest peñol on the Antioquian batholith, the Guatapé peñol, is located between the towns of El Peñol and Guatapé. In plan it measures 290 by 75 meters and is 130 meters high (Fig.2) (BOTERO A., 1963, p. 29).

4.3. TOPOGRAPHY AND OUTCROPS

Topography on the Antioquian batholith is mostly mature and characterized by monotonous successions of rounded hills. Local relief is mostly 400 m or less, although major rivers suchs as the Porce, Nare, Guatapé and others have cut canyons considerably deeper. Greater local relief, in places more than 500 m is developed in the north between

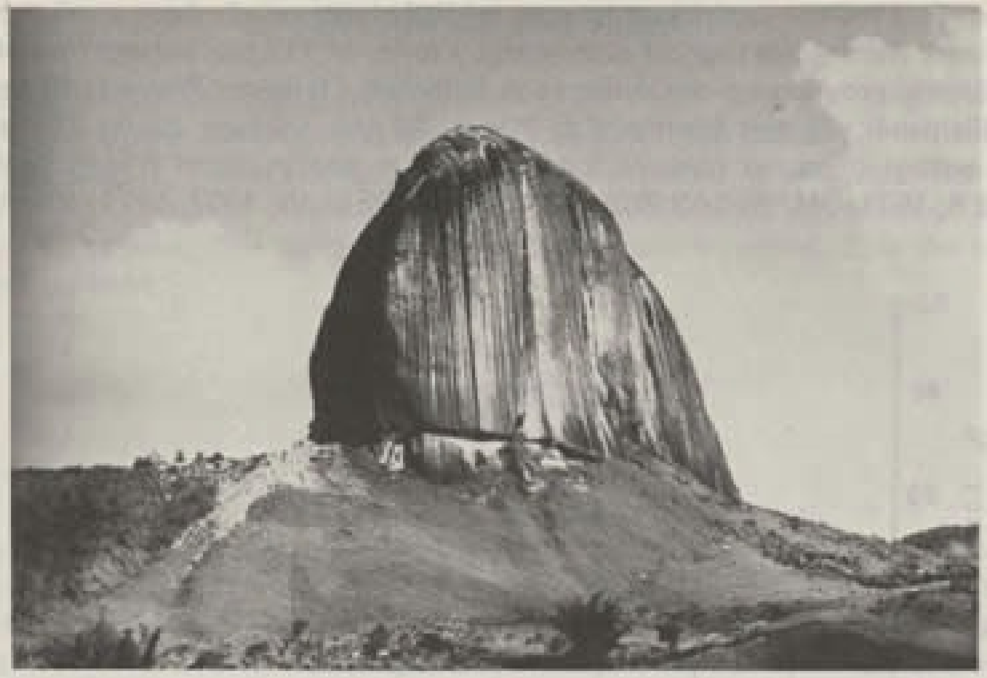

FIGURE 2. The Guatapé Peñol.

Guadalupe and Amalfi, and the south near San Luis. Relief on surrounding host rock is everywhere greater than on the adjacent batholith. Large areas of nearly flat topography, locally covered by rotted late Tertiary (?) and Quaternary (?) gravels, is developed around Rionegro, east of Medellín.

Outcrops of fresh batholith rock are scarce. They are largely restricted to stream beds and are decidedly less abundant than outcrops of surrounding host rock. Only in steep tributaries to major rivers, especially the Nus, Guatapé and San Carlos, are outcrops both large and abundant. Some of these difficultly accesible outcrops have areas of serveral thousand square meters.

Peñoles afford enormous exposures of fresh rock but they are not numerous. The Guatapé **peñol** is accompanied by several smaller ones in the same area. Others dominate the towns of Entrerrios and San Carlos.

By far the majority of our samples have come from the nearly ubiquitous residual boulders of fresh rock left behind during the secular weathering of the batholith. Many of these boulders are in place as they are encased in the rotted rock which preserves perfectly the texture of fresh rock. Others have doubtlessly, crept slid, or rolled down slope to accumulate in gullies and stream valleys, accumulations locally known as **organales** (BOTERO, A., 1963, p. 32). Yet, none sampled are believed to be far travelled (more than a few hundred meters) and such small transport would little affect the conclusions of this study.

5. REGIONAL GEOLOGY AND GEOGRAPHY OF THE COLOMBIAN ANDES

The Andes enter Colombia from the south as a single cordillera. Just north of the Ecuatorian border, this cordillera splits twice to form three subparallel ranges which constitute the Western, Central and Eastern Cordilleras of the Colombian Andes. The three cordilleras are separated by the valleys of the Cauca and Magdalena rivers.

The entire Magdalena valley and much of the Cauca valley are structural depressions extensively filled with Middle and Upper Tertiary, non-marine, clastic sedimentary rocks (GROSSE, 1926; VAN HOUTEN and TRAVIS, 1968).

The Western Cordillera is composed chiefly of intensely deformed but nonmetamorphic Cretaceous and Lower Tertiary (?) eugeosynclinal ophiolitic and trench assemblage sedimentary and mafic volcanic rocks (IRVING, 1971; BARRERO, 1979). Locally these rocks are host to stocks and batholiths of Tertiary age that range principally from quartz diorite to diorite. Phyllite and low grade schist of possible Paleozoic age (NELSON, 1957) occur sporadically. To the north, the Western Cordillera breaks up into a series of low ranges that die out short of the Caribbean coast. An offshoot range, the Serranía de Baudó, passes northwestward into Panamá along the Pacific coast east of the Gulf of Urabá (CASE, and others, 1971).

The Eastern Cordillera is the non-volcanic, possibly back-arc assemblage counterpart of the Western Cordillera and is composed of folded and faulted Cretaceous and Lower Tertiary clastic sedimentary rocks of great aggregate thickness (CAMPBELL and BURGL, 1965; McLAUGHLIN, 1972). These rocks are locally interrupted by massifs of older sedimentary and crystalline rocks that range in age from Precambrian to Jurassic (RADELLI, 1962; RENZONI, 1965; STIBANE, 1968 WARD, and others, 1969). To the north, near the Venezuelan border, the Eastern Cordillera bifurcates to form the Serranía de Perijá and the Mérida Andes which together bound the Maracaibo Basin on the west and southeast, respectively.

The Central Cordillera is the home of Colombia's major Andean batholiths, the largest and northernmost of which is the Antioquian batholith. These batholiths are the root remnants of what was an extensive volcanic arc in Cretaceous time. Modern arc deposits in Colombia are less widespread. They are confined to the belt of volcanos and associate lavas and pyroclastic deposits astride the southern Central Cordillera. Other rocks in the Central Cordillera are chiefly metamorphic rocks of Paleozoic (and locally Precambrian) age (GROSSE, 1926, POSADA, 1936, BOTERO, A., 1941, 1942; NELSON, 1962; FEININGER, and others, 1970) These rocks are in places overlain by patches of marine sedimentary and volcanic rocks of Middle Cretaceous age (FEININGER, and others, 1970; ALVAREZ, HALL and others, 1970). North of the city of Medellín the altitude of the Central Cordillera dimishes progressively, and within 300 km the cordillera is lost beneath Holocene alluvium of the Cauca and Magdalena rivers where their valleys merge.

The Sierra Nevada de Santa Marta massif on Colombia's north coast east of Barranquilla stands in isolated splendor with summit elevations 5900 m only 45 km from the Caribbean shore. The massif is an enormous horst, triangular in plan, composed chielfly but not exclusively of cristallyne rocks (TSCHANZ, and others, 1969). The massif has not been affected by young volcanism. Its relations to the three Andean cordilleras of Colombia is uncertain.

6. HOST ROCKS TO THE ANTIOQUIAN BATHOLITH

Host rocks to the Antioquian batholith are chiefly gneiss, schist, and phyllite of Paleozoic age with lesser areas of highly deformed but nonmetamorphic Cretaceous eugeosynclinal sedimentary and volcanic rocks and a belt of serpentinite at Medellín (see INVENTARIO MINERO NACIONAL, 1965; FEININGER, and others, 1970; ALVAREZ, J., HALL, and others, 1970). Other rocks cut by the batholith are plutons of Cretaceous age that range from quartz monzonite to gabbro. The felsic plutons are mediun grained and massive to gneissic. The gabbro is extensively saussuritized and uralitized. The largest body, northeast of Yarumal, has a core of serpetinite 2 km^2 in area.

The Paleozoic rocks underwent a low-pressure facies series regional metamorphism prior to emplacement of the Antioquian batholith. The grade of metamorphism ranges from low greenschist facies in phyllite around Amalfi and northeast of San Luis, to middle amphibolite facies in gneiss with muscovite, andalusite, and sillimanite along much of the east border of the batholith north of the latitude of San Carlos, and southeast of Medellín. Many mineralogical characteristics of the metamorphic rocks are like those produced by shallow thermal metamorphism. Nevertheless, the absence of an orderly relationship between the batholith contact and the spatial distribution of metamorphic facies shows that metamorphism must predate and therefore be unrelated to the Antioquian batholith.

Thermal metamorphism by the Antioquian batholith overprinted on the earlier regional metamorphism can be recognized in many places. Stout prisms of sillimanite are developed in phyllite adjacent to the batholith southeast of San Carlos. Feldspathic gneiss near the batholith commonly has porphyroblasts of cordierite with inclusions of spinel, and in marble the development of wollastonite is widespread. Sillimanite gneiss has been developed adjacent to the batholith at the tunnel on the new Medellín - Bogotá Road east of Copacabana.

7. THE ANTIOQUIAN BATHOLITH

7.1. GENERAL STATEMENT

Recent studies of the Sierra Nevada batholith in California (BATEMAN, and others, 1963; BATEMAN and EATON, 1967; ROSS, 1969; EVERNDEN and KISTLER, 1970, KISTLER, EVERNDEN and SHAW, 1971) have successfully unravelled many petrological and structural riddles of that great batholith. Nevertheless, the profusion of literature on the Sierra Nevada batholith should not cast a constructive shadow across geologic thinking applied to other circum-Pacific batholiths. In fact, the reader who is familiar with the Sierra Nevada reports cited above will be inmediately struck by the marked dissimiliarities between the Antioquian batholith and its distant neighbor to the north.

Rocks of the Antioquian batholith were first noted century and a half ago by Boussingault (1825). Later workers (OSPINA, 1911; SCHEIBE, 1933; POSADA, 1936) stressed the great regional extent of granitic rocks and added petrographic details, but it was not until 1942 thart Botero recognized the nature of the Antioquian batholith and gave it its name. Nearly the entire batholith is now covered by published geologic maps (BOTERO, A., 1963 INVENTARIO MINERO NACIONAL, 1965; FEININGER, and others, 1970;

ALVAREZ, J, HALL, and others, 1970) but none of these are readily available outside of Colombia.

The Antioquian Batholith has an exposed area of 7221 km^2 (2788 mi^2, or 21 percent larger than the Boulder batholith, Montana and more than half as large as the State of Connecticut, U.S.A.). Satellite stocks believed consanguinous with the Antioquian Batholith add at least 322 km^2 (124 mi^2).

The outstanding characteristic of the Antioquian batholith is its remarkable homogeneity: 97 percent (7003 km^2) of the batholith is composed of monotonously uniform quartz diorite or granodiorite that differs but little or not at all from place to place. This rock is here referred to as the normal facies. Two subordinate facies, one felsic and the other gabbroic, have also been recognized (Fig. 3).

7.2. AGE

Stratigraphically, the age of the batholith can be fixed only imprecisely. The youngest rocks cut by the batholith are eugeosynclinal sedimentary and volcanic rocks of Cretaceous age. These contain Early Cretaceous (Albian and Aptian) marine fossils at a number of localities not far from the batholith contact (FEININGER, and others, 1972). The oldest rock that unconformably overlies the batholith is alluvium of Quaternary age.

During the past decade, potassium-argon biotite ages have been determined on a number of samples from the Antioquian batholith. The ages obtained range from 58 to 83 m.y. (Table 2) and indicate a later Cretaceous age.

The small spread of ages of these widely spaced samples (see Fig. 3) is in accord with the unusual petrographic uniformity of the batholith.

7.3. PETROGRAPHY

7.3.1. NORMAL FACIES

Rock of the normal facies of the Antioquian batholith is medium - to coarse - grained, massive, hypidiomorphic equigranular, gray quartz diorite or granodiorite (rarely quartz monzonite) with a pronounced salt-and- pepper texture. It is composed of white to light gray feldspar, gray vitreous quartz, deep green to black hornblende, brown to black

TABLE 2.

RADIOMETRIC AGES (BIOTITE) OF SAMPLES FROM THE ANTIOQUIAN BATHOLITH AND A CONSANGUINOUS STOCK

Location of sample (Coordinates) X	Y	Z	Method.	Age (m.y.)	Comment	Reference
1,213,750	852,750	2,200	K/Ar	79 ± 3		Botero A., 1963, p.81
1,243,500	863,750	1,950	K/Ar	74 ± 3		Pérez A., 1967
1,233,250	831,250	2,600	K/Ar	72 ± 3		Pérez A., 1967
1,200,000	830,000	2,700	K/Ar	70 ± 3	Consaguinous stock	Pérez A., 1967
1,185,750	866,250	1,600	K/Ar	71 ± 3		Pérez A., 1967
1,160,000	898,000	1,200	K/Ar	83 ± 3		Pérez A., 1967
1,216,500	925,500	925	K/Ar	68 ± 2	Felsic facies	Prof. Bruno J. Giletti, written commun. 1967
1,200,000	854,000	2,025	Rb/Sr	60	Cataclastic rock "near Don Matías".	Fujiyoshi et al., 1976
1,200,000	854,000	2,025	Rb/Sr	58	Cataclastic rock "near Don Matías".	Fujiyoshi et al., 1976
1,262,000	852,000	2,300	Rb/Sr	68	Yarumal	Fujiyoshi et al., 1976

biotite, and accessory minerals. Modal analyses and other properties of 214 samples of normal facies rocks spaced over the entire batholith (Fig. 3) are given in Table 3. The small standard deviation for each of the major minerals underscores the unusual uniformity of the normal facies. Chemical analyses of two samples are given in Table 4.

Plagioclase, chiefly andesine, constitutes nearly half the normal facies rock. Grains are subhedral to euhedral, well twinned, and generally fresh. Normal zoning with oscillatory reversals is common, although strongly zoned, weakly zoned, and even unzoned crystals may occur in a single thin section. Small inclusions of hornblende and clinopyroxene are prominent inclusions in the cores of some plagioclase grains (Fig. 4). Rare grains have small cores of calcic bytownite in sharp contact with surrounding andesine. In cataclastic rock patches of plagioclase commonly have been replaced by potassium feldspar.

Quartz forms clean anhedral grains and interstitial fill in small optically continous domains (Fig. 5). Undulatory extinction is not normally conspicuous, and in 20 percent of the samples studied, quartz shows no evidence of deformation.

TABLA 3

MODAL ANALYSES AND OTHER PROPERTIES OF 214 SAMPLES OF THE NORMAL FACIES, ANTIOQUIA BATHOLITH

No.	1. FIELD NUMBER	COORDINATES (2) 2. X	3. Y	4. Z	5. QUARTZ	6. K FELDSPAR	7. PLAGIOCLASE	8. HORNBLENDE	9. CLINOPIROXENE	10. BIOTITE	11. CHLORITE	12. BIOTITE + CHLORITE	13. ALLANITE	14. APATITE	15. CALCITE	16. EPIDOTE	17. OPAQUE	18. PREHNITE	19. SPHENE	20. ZIRCON	21. TOTAL	22. An CONTENT OF PLAGIOCLASE	23. COLOR INDEX	24. DEFORMATIONS	25. SPECIFIC GRAVITY	26. CLASSIFICATIONS	27. No. OF POINTS OF LENGTH OF TRAVERSE (8)	28. REMARKS
1	7825	1,207,350	933,350	600	22.8	9.3	55.7	1.4	—	8.1	2.3	10.4	—	0.1	T(6)	T	0.1	—	0.2	T	100.0	40	12.1	1	2.73	GD	1717P	
2	7824	1,208,000	927,850	725	27.3	0.5	56.8	5.6	—	4.0	4.2	8.2	—	0.2	0.7	0.2	T	—	0.5	T	100.0	41	14.5	1	2.78	QD	1207P	Sample 180m from contact
3	7610	1,211,850	923,750	775	23.0		49.5	—	—	—	22.4	22.4	—	0.4	3.2	0.9	0.4	—	0.1	0.1	100.0	43	23.8	1	2.75	QD	1362P	Chlorite: 15.3%from biotite 7.1 from hornblende.
4	7966	1,196,250	921,950	750	19.8	0.2	53.0	18.0	0.6	2.7	5.0	7.7	—	0.4	—	—	0.2	—	0.1	T	100.0	43	26.6	1	2.82	QD	1177P	Sample 500 m from contact
5	7980	1,199,400	921,100	725	20.4	9.0	46.6	11.9	0.3	—	10.1	10.1	T	0.2	0.4	0.9	T	—	0.1	0.1	100.0	39	23.3	—	2.77	GD	1723P	Sample 50 m from contact
6	7968	1,190,000	920,600	500	21.8	8.4	56.1	4.6	0.1	1.9	6.3	8.2	—	T	0.1	0.4	T	0.2	0.1	T	100.0	—	13.4	0	2.70	GD	1028P	From Nare fault.
7	7969	1,190,400	920,100	500	17.9	0.7	56.4	10.3	—	7.5	6.5	14.0	T	0.1	0.2	T	0.1	0.1	0.2	T	100.0	43	24.6	1	2.80	QD	1556P	From Nare fault.
8	7908	1,195,900	919,600	825	21.4	1.6	45.5	9.3	1.3	20.7	—	20.7	T	0.2	—	—	T	—	T	T	100.0	44	31.3	1	2.82	QD	1137P	Weak platy flow structure; tourmaline, T
9	7761	1,241,700	919,500	1,025	31.3	17.9	40.1	3.4	—	4.3	2.4	6.7	T-	T	—	0.1	0.5	—	T	T	100.0	45	11.6	0	2.72	GD	1000P	
10	8086	1,176,100	918,400	525	20.2	7.2	52.4	6.4	—	10.4	1.9	12.3	0.1	0.2	—	0.2	0.6	0.1	0.3	T	100.0	42	19.9	0	2.74	GD	1227P	
11	7965	1,191,800	918,050	500	27.2	8.0	49.7	5.6	—	2.3	5.7	8.0	—	0.1	—	0.8	0.4	—	0.2	T	100.0	43	15.0	2	2.76	GD	2108	From Nare fault.
12	7957	1,181,950	917,850	825	23.8	8.4	52.6	3.7	—	8.6	1.9	10.5	—	0.1	T	0.1	0.8	—	T	T	100.0	39	15.1	1	2.76	GD	1230P	
13	7707	1,247,500	917,250	1,150	15.7	5.3	58.1	9.3	0.1	7.9	2.4	10.3	T	T	—	0.5	0.5	—	T	T	99.8	46	20.7	1	2.78	QD	621P	Sample 100 m from contact
14	7975	1,200,750	916,550	875	25.6	11.4	42.7	10.1	0.2	8.5	1.0	9.5	0.1	0.2	—	0.1	0.1	—	T	T	100.0	42	20.1	1	2.78	GD	1516P	
15	7542	1,234,750	916,100	1,100	14.8	12.3	55.8	8.1	0.1	7.7	0.5	8.2	—	T	—	T	0.7	—	—	T	100.0	46	17.1	1	2.79	GD	979P	
16	7555	1,221,000	916,100	1,075	21.3	5.1	55.5	5.4	T	6.5	4.7	11.2	—	0.2	—	0.5	0.2	—	0.6	T	100.0	42	17.9	0	2.76	QD	1306P	
17	7976	1,200,650	916,050	875	24.4	10.0	41.7	5.4	—	1.8	8.8	10.6	T	0.1	6.5	0.1	1.2	—	T	T	100.0	447	17.3	2	2.74	GD	1873P	Chlorite derived from both biotite and hornblende.
18	2681	1,178,800	915,550	725	25.2	4.2	53.0	7.0	—	8.1	1.1	9.2	0.1	0.2	T	0.1	0.8	0.1	0.1	T	100.0	41	17.3	0	—	QD	1960P	
19	7608	1,218,200	915,500	1,075	25.8	4.6	45.6	16.2	—	5.3	0.5	5.8	—	0.1	—	0.5	1.3	—	0.1	T	100.0	49	23.9	1	2.79	QD	1428P	
20	7612	1,216,800	915,300	975	23.3	0.3	53.2	5.0	—	17.7	0.1	17.8	—	0.1	—	0.3	T	—	T	T	100.0	46	23.1	1	2.80	QD	1449P	Weak platy flow structure.
21	7992	1,229,600	915,000	1,175	25.4	8.8	55.8	7.7	T	1.9	T	1.9	—	0.1	—	—	0.2	—	0.1	T	100.0	44	10.0	1	2.75	GD	1473P	
22	7550	1,225,000	913,100	1,200	27.1	21.2	43.9	2.4	—	4.8	T	4.8	—	0.3	—	0.1	0.1	—	0.1	T	100.0	42	7.5	1	2.73	GD-	1346P	Weak platy flow structure.
23	7664	1,237,150	913,050	1,250	26.4	14.0	44.4	6.2	T	8.9	—	8.9	T	T	—	—	0.1	—	—	T	100.0	55	15.2	0	2.75	GD	1000P	
24	7716	1,237,150	912,900	1,275	27.7	11.4	38.6	7.8	0.2	13.3	0.1	13.4	—	0.1	—	T	0.7	—	—	0.1	100.0	45	22.1	0	2.74	GD	1000P	
25	7715	1,237,150	912,000	1,275	22.9	1.9	57.4	9.9	—	5.0	1.3	6.3	—	0.1	—	0.6	0.8	—	T	T	99.9	47	17.6	O	2.78	QD	1000P	
26	7606	1,211,400	911,500	875	18.3	1.6	45.1	18.5	1.0	15.2	—	15.2	—	0.2	—	T	T	—	—	0.1	100.0	46	34.7	0	2.82	QD	1392P	Moderate platy flow structure.
27	7971	1,204,800	911,450	925	27.5	6.1	51.6	3.4	—	9.2	0.3	9.5	—	0.1	—	1.2	0.3	—	0.3	T	100.0	43	14.7	1	2.77	GD	1216P	K feldspar a Microcline.
28	7523	1,238,750	911,100	1,325	23.0	16.8	46.8	6.9	T	5.2	0.5	5.7	—	0.2	—	0.1	0.4	—	—	0.1	100.0	49	13.1	0	2.76	GD	1413P	
29	7962	1,196,000	910,250	800	19.5	8.0	49.1	14.9	0.6	7.2	0.5	7.7	T	0.2	—	—	T	—	T	T	100.0	42	23.2	1	2.80	GD	1385P	Weak platy flow structure.
30	7852	1,196,700	909,600	700	25.1	9.3	44.4	12.0	0.1	7.9	0.6	8.5	—	0.1	—	0.3	0.2	—	T	T	100.0	41	21.1	0	2.76	GD	1777P	Weak platy flow structure.
31	8538	1,174,950	909,050	1,050	24.6	1.1	54.6	3.7	0.1	12.6	2.0	14.6	T	0.4	0.4	0.1	0.4	—	T	T	100.0	38	18.9	0	2.78	QD,	1622P	Sample 50 m from contact
32	8526	1,207,150	908,900	925	27.3	10.9	43.1	4.6	—	10.1	0.9	11.0	—	0.2	—	2.0	0.1	—	0.8	T	100.0	39	18.5	—	2.77	GD	6000P	Near Cristales shear zone
33	7811	1,254,250	908,700	1,000	26.3	1.4	54.2	5.8	—	11.2	0.9	12.1	[illegible]	T	—	0.1	T	—	0.1	T	100.0	43	18.1	0	2.79	QD	1000P	
34	8239	1,178,400	908,450	925	27.6	23.4	35.7	5.3	—	7.4	0.1	7.5	[illegible]	T	—	—	0.4	—	—	T	99.9	44	13.2	0	2.71	QM	1095P	Some plagioclases have very calcic cores

No.	1. FIELD NUMBER	COORDINATES (2) 2. X	3. Y	4. Z	5. QUARTZ	6. K FELDSPAR	7. PLAGIOCLASE	8. HORNBLENDE	9. CLINOPYROXENE	10. BIOTITE	11. CHLORITE	12. BIOTITE + CHLORITE	13. ALLANITE	14. APATITE	15. CALCITE	16. EPIDOTE	17. OPAQUE	18. PREHNITE	19. SPHENE	20. ZIRCON	21. TOTAL	22. An CONTENT OF PLAGIOCLASE	23. COLOR INDEX	24. DEFORMATION (3)	25. SPECIFIC GRAVITY	26. CLASSIFICATION (4)	27. No. OF POINTS OR LENGTH OF TRAVERSE (5)	28. REMARKS
35	7695	1,255,400	908,300	1,100	20.8	6.2	51.7	9.0	0.7	10.4	0.9	11.3	T	0.2	T	–	T	–	T	T	100.0	45	21.1	0	2.80	GD	1000P	Sample 20 m below roof of batholith
36	8527	1,209,900	908,200	1,000	21.8	4.9	52.6	10.3	–	10.0	0.1	10.1	–	0.1	–	–	T	–	0.2	T	100.0	47	20.6	1	2.82	QD	2800P	Foliated; near Cristales shear zone
37	7947	1,187,950	908,200	1,125	18.4	0.4	63.6	4.2	–	10.4	1.5	11.9	–	0.1	0.3	0.7	0.1	0.1	0.2	T	100.0	46	17.1	0	2.79	QD	1237P	Sample about 10 m below roof of batholith
38	7909	1,207,800	907,700	975	24.0	3.5	42.1	9.1	–	19.4	0.4	19.8	–	0.2	–	0.1	0.6	–	0.5	0.1	100.0	44	30.1	2	2.77	QD	983P	
39	7568	1,217,250	907,300	1,250	21.8	7.7	45.4	11.6	1.5	11.5	0.1	11.6	–	0.2	–	–	0.1	–	0.1	T	100.0	48	24.9	1	2.81	GD	1441P	Strong platy flow structure
40	7894	1,180,950	907,200	850	15.4	0.6	68.7	2.7	–	9.6	1.2	10.8	–	0.3	–	0.1	1.2	–	0.2	T	100.0	38	15.0	0	2.77	QD	1275P	
41	7544	1,225,200	906,800	1,125	13.8	3.0	56.1	17.4	0.2	5.8	2.0	7.8	–	0.2	–	0.2	0.4	–	0.8	0.1	100.0	40	26.8	1	2.82	QD	1214P	Interstitial hornblende
42	7682	1,251,400	906,250	1,225	23.3	8.0	55.9	4.4	–	5.5	2.4	7.9	–	0.1	–	0.1	0.1	–	0.1	0.1	100.0	39	12.6	0	2.73	GD	1000P	
43	7745	1,240,200	905,400	1,350	22.4	0.1	56.9	6.4	–	13.1	1.0	14.1	T	T	–	–	0.1	–	T	T	100.0	42	20.6	0	2.75	QD	1000P	Sample 50 m from contact.
44	7895	1,182,600	904,600	1,125	20.6	9.6	43.7	13.3	1.2	9.4	1.3	10.7	T	0.1	T	0.4	0.1	T	0.3	T	100.0	43	26.0	0	2.79	GD	1543P	
45	7855	1,196,000	904,500	1,050	20.6	8.3	51.3	9.6	T	7.8	1.6	9.4	–	0.2	–	0.1	0.4	–	0.1	T	100.0	42	19.6	0	2.78	GD	1500P	Weak platy flow structure.
46	8138	1,155,350	904,100	375	18.9	8.8	58.1	4.3	0.2	7.8	1.1	8.9	–	0.2	–	0.1	0.3	T	0.1	0.1	100.0	42	13.9	1	2.73	GD	1293P	Sample < 10m from contact
47	7941	1,174,300	903,400	1.100	25.3	1.2	49.0	7.9	–	16.3	0.2	16.5	–	0.1	T	–	T	–	–	T	100.0	47	24.4	1	2.80	QD	1034P	
48	8680	1,241,700	902,550	1,300	19.6	5.0	53.8	12.5	1.3	6.7	0.9	7.6	–	0.1	–	T	0.1	–	–	T	100.0	46	21.5	0	2.82	QD	913P	Interstitial hornblende; sample 100 m from contact.
49	8012	1,159,200	902,550	875	22.0	8.8	45.5	9.9	1.6	10.3	1.2	11.5	0.1	0.3	–	–	0.2	T	–	0.1	100.0	49	23.3	1	2.77	GD	1794P	
50	7998	1,161,850	901,950	1,125	28.4	11.2	47.8	5.5	T	3.8	2.7	6.5	–	0.1	–	–	0.1	0.1	0.3	T	100.0	43	12.4	0	2.76	GD	1450P	
51	7528	1,220,700	901,550	1,275	23.8	9.4	51.2	7.4	–	5.7	1.2	6.9	0.1	0.1	–	0.2	0.6	–	0.3	–	100.0	43	15.5	0	2.75	GD	1356P	Weak platy flow structure
52	7942	1,176,650	901,350	1,025	23.2	10.8	43.6	10.1	0.1	11.5	0.2	11.7	–	0.3	T	–	0.1	–	0.1	T	100.0	42	22.0	1	2.76	GD	1242P	
53	7853	1,191,200	901,300	1,025	22.3	9.8	56.0	9.3	0.1	1.3	0.3	1.6	–	T	0.1	0.1	0.6	–	0.1	T	100.0	43	11.8	1	2.77	GD	1849P	
54	7854	1,192,250	900,950	1,000	25.3	10.1	47.4	8.1	T	6.3	1.9	8.2	–	T	–	0.4	0.2	–	0.2	0.1	100.0	40	17.1	1	2.77	GD	1682P	
55	7733	1,210,750	900,700	1,100	28.6	7.9	45.8	–	–	7.5	T	7.5	–	T	–	0.8	0.6	–	0.1	–	100.0	41	17.7	2	2.75	GD	1000P	K Feldespar is microcline; some hornblende replaced by biotite; from Sofía shear zone
56	8392	1,229,500	900,050	1,200	28.6	5.9	53.8	–	–	–	7.0	7.0	T	0.1	0.2	1.0	0.5	0.2	0.1	T	100.0	37	11.2	1	2.72	QD	1745P	Hornblende partly chloritized
57	7668	1,253,600	89,550	1,600	23.5	10.7	45.0	10.0	0.6	10.0	–	10.0	–	T	–	0.2	T	–	–	–	100.0	44	20.8	0	2.80	GD	391P	Sample 5 m below roof of batholith
58	7667	1,253,600	89,550	1,600	18.6	3.2	47.0	10.3	0.3	17.0	2.6	19.6	T	0.1	T	T	T	–	0.9	T	100.0	46	31.1	1	2.80	QD	689P	Sample 15 m below roof of batholith
59	8681	1,247,900	899,300	1,600	21.0	7.5	46.2	14.3	0.5	7.5	2.2	9.7	–	0.1	0.1	0.1	0.3	–	0.2	T	100.0	46	25.1	0	2.81	GD	1480P	K feldspar in part microcline
60	7505	1,221,350	899,050	1,475	26.0	3.8	48.2	4.5	–	15.2	1.0	16.2	–	0.1	–	0.5	0.4	–	0.3	T	100.0	43	21.9	1	2.74	QD	1000P	
61	8390	1,201,200	898,250	1,225	25.0	15.5	42.9	12.9	T	2.4	0.3	2.7	–	0.2	–	T	0.4	–	0.4	T	100.0	42	16.4	1	2.76	GD	1072P	
62	8389	1,204,900	897,700	1,450	14.6	0.3	46.3	25.4	T	10.0	1.3	11.3	–	0.1	–	1.2	0.6	–	0.3	–	100.0	50	38.8	0	2.89	QD	1190P	
63	8543	1,168,800	897,500	1,475	24.4	7.4	51.9	6.4	0.3	9.2	0.3	9.5	–	0.1	–	T	T	–	T	T	100.0	43	16.2	1	2.78	GD	1220P	
64	7997	1,162,500	897,500	1,250	23.5	7.4	42.8	12.4	1.7	11.4	0.2	11.6	T	0.3	0.1	0.1	0.1	–	–	–	100.0	45	25.9	0	2.79	GD	1575P	
65	7946	1,188,900	897,050	1.000	22.6	10.5	46.4	10.8	–	6.4	1.8	8.2	–	0.1	–	0.6	0.5	–	0.3	T	100.0	43	20.4	1	2.78	GD	1705P	

No.	1. FIELD NUMBER	COORDINATES (2) 2. X	3. Y	4. Z	5. QUARTZ	6. K FELDSPAR	7. PLAGIOCLASE	8. HORNBLENDE	9. CLINOPYROXENE	10. BIOTITE	11. CHLORITE	12. BIOTITE + CHLORITE	13. ALLANITE	14. APATITE	15. CALCITE	16. EPIDOTE	17. OPAQUE	18. PREHNITE	19. SPHENE	20. ZIRCON	21. TOTAL	22. An CONTENT OF PLAGIOCLASE	23. COLOR INDEX	24. DEFORMATION (3)	25. SPECIFIC GRAVITY	26. CLASSIFICATION (4)	27. No. OF POINTS OR LENGTH OF TRAVERSE (5)	28. REMARKS
66	7991	1,216,550	896,400	1,225	24.3	7.4	51.0	10.4	–	4.3	1.1	5.4	0.2	0.1	T	0.3	0.8	–	0.1	T	100.0	46	17.2	1	2.77	GD	1677P	
67	8017	1,157,050	896,300	1,450	27.5	16.9	36.9	9.3	0.4	7.6	1.0	8.6	–	0.1	–	–	0.1	–	0.1	0.1	100.0	46	18.5	0	2.73	GD	1572P	Sample <100 m below roof of batholith
68	7937	1,184,650	894,950	1,000	28.8	12.5	40.2	11.2	–	–	5.7	5.7	–	T	1.1.	0.3	0.1	–	0.1	T	100.0	43	17.4	1	2.71	GD	1217P	From Bizcocho fault.
69	8541	1,178,750	894,800	1,450	26.2	–	42.5	1.7	–	13.9	0.1	14.0	0.1	0.1	–	–	0.4	–	–	T	100.0	40	16.2	1	2.71	GD	1500P	Plagioclase partly replaced by K feldspar
70	7936	1,191,950	894,700	1,025	26.1	10.5	43.1	8.5	0.2	9.1	1.8	10.9	–	0.2	–	0.2	0.2	–	0.1	T	100.0	42	20.1	0	2.77	GD	1300P	
71	7938	1,181,850	893,900	1,225	27.2	1.2	52.3	6.5	–	10.9	0.4	11.3	–	0.3	–	0.3	0.5	–	0.4	T	100.0	43	19.0	1	2.80	QD	1341P	
72	7522	1,220,400	893,500	1,450	28.7	19.8	39.4	5.3	–	3.2	3.0	6.2	–	T	–	0.3	0.3	–	T	–	100.0	45	12.1	1	2.69	GD	1000P	
73	7880	1,241,800	893,400	1,500	31.4	4.9	48.1	4.4	–	8.3	2.1	10.4	0.1	0.1	–	0.3	0.1	T	0.1	0.1	100.0	43?	15.4	1	2.71	QD	1506P	
74	7726	1,214,000	892,500	1,000	25.0	1.2	57.8	8.6	–	4.6	1.2	5.8	–	T	–	1.0	0.4	–	0.2	–	100.0	38	15.1	1	2.79	QD	500P	
75	7999	1,166,250	891,900	1,375	26.6	15.0	46.1	2.8	–	8.3	0.1	8.4	–	0.1	–	0.5	0.1	–	0.4	T	100.0	43?	12.2	1	2.70	GD	1048P	
76	8542	1,172,400	891,350	1,400	25.0	12.8	54.4	2.3	–	4.1	0.1	4.2	–	0.1	–	–	1.0	–	0.2	T	100.0	40	7.7	2	2.70	GD	1228P	
77	8008	1,161.750	890,850	975	23.6	13.8	43.3	7.0	–	0.1	10.4	10.5	–	T	–	1.3	T	–	0.5	T	100.0	39	19.3	2	2.74	GD	1142P	
78	8009	1,161,600	890,700	975	25.8	9.7	40.6	10.9	0.2	4.3	7.3	11.6	T	0.2	–	0.5	T	–	0.5	T	100.0	43	23.7	2	2.77	GD	1054P	
79	7933	1,188,200	890,600	1,050	25.6	–	49.6	7.2	–	–	11.7	11.7	–	0.1	–	1.1	0.1	–	1.7	0.1	100.0	43	21.8	–	2.75	QD	1399P	From Bizcocho fault; plagioclase partly replaced by K feldspar
80	7556	1,219,350	890,550	1,475	19.2	8.0	52.9	12.4	–	0.1	5.7	5.8	–	0.2	–	1.1	0.3	–	0.1	T	100.0	41	19.7	2	2.80	GD	1263P	
81	8388	1,204,950	890,350	1,450	23.6	9.8	50.4	5.5	T	8.4	1.3	9.7	–	0.2	–	0.2	0.2	–	0.4	T	100.0	46	16.0	1	2.77	GD	1255P	
82	7605	1,215,600	890,200	1,175	25.3	14.7	45.6	3.3	–	–	7.4	7.4	–	0.2	1.5	0.2	0.9	–	0.9	T	100.0	40	12.7	1	2.71	GD	1888P	
83	7720	1,224,000	890,150	1,425	26.1	12.8	47.1	1.1	T	12.0	0.2	12.2	–	0.2	T	0.1	0.4	T	T	T	100.0	40	13.8	1	2.75	GD	922P	
84	7604	1,216,150	890,000	1,425	24.6	15.9	43.9	7.0	0.3	3.7	3.0	6.7	–	0.3	–	0.4	0.5	–	0.3	0.1	100.0	45	15.2	1	2.72	GD	1878P	
85	8061	1,157,100	889,000	700	26.8	14.7	41.9	5.3	–	0.8	8.8	9.6	–	0.1	0.1	1.2	T	–	0.3	T	100.0	40	16.4	2	2.73	GD	1426P	K feldespar is microcline.
86	8129	1,164,700	888,950	1,075	24.3	14.6	42.0	8.8	T	9.4	0.3	9.7	T	0.4	–	0.2	T	–	T	T	100.0	42	18.7	2	2.76	GD	1283P	K feldespar in part microcline.
87	8381	1,199,300	888,750	1,475	22.5	4.6	50.7	4.6	–	16.8	0.2	17.0	–	0.2	–	–	0.3	–	0.1	T	100.0	37?	22.0	2	2.76	QD	1316P	
88	7858	1,246,750	888,300	1,775	18.8	3.1	53.6	12.2	T	11.5	0.6	12.1	–	0.1	–	–	T	–	0.1	T	100.0	50	24.4	0	2.80	QD	1930P	Sample 5 m below roof of batholith.
89	7857	1,247,300	888,200	1,725	21.2	4.7	51.8	8.5	0.2	11.5	0.5	12.0	–	0.1	–	0.1	1.3	–	0.1	T	100.0	46	22.2	0	2.78	QD	2109P	Sample 45 m below roof of batholith.
90	8679	1,244,950	887,950	1,725	28.3	3.2	52.1	6.0	–	8.6	0.3	8.9	T	T	–	0.2	1.1	–	0.2	T	100.0	46	16.4	1	2.79	QD	652P	
91	7934	1,186,400	886,700	1,350	27.7	5.1	50.3	6.5	–	8.7	1.2	9.9	0.2	0.2	–	0.1	T	–	–	T	100.0	48	16.7	2	2.77	QD	1226P	
92	8010	1,169,200	886.550	1,825	26.7	7.9	40.1	5.6	–	19.3	0.1	19.4	0.1	T	–	–	0.2	–	T	T	100.0	37	25.3	2	2.75	GD	1017P	
93	2680	1,170,150	886,450	1,925	24.4	9.0	43.6	10.4	0.1	11.7	0.3	12.0	–	0.2	T	–	0.2	–	0.1	T	100.0	46	22.8	1	–	GD	1780P	
94	8019	1,177,150	886,000	1,975	23.6	13.5	44.4	12.8	T	4.9	0.6	5.5	0.1	T	–	–	0.1	–	T	T	100.0	48	18.5	2	2.77	GD	1040P	
95	7757	1,235,300	885,850	975	23.4	9.9	51.7		–	–	13.4	13.4	–	0.1	–	1.4	0.1	–	T	–	100.0	33?	14.9	2	2.71	GD	1000P	Chlorite from biotite and hornblende
96	7500	1,219,300	884.550	1,625	28.3	9.8	43.4	10.8	0.3	5.6	0.9	6.5	–	T	–	T	0.8	T	–	–	99.9	43	18.4	0	2.76	GD	2000P	
97	7666	1,215,100	884.200	1,375	24.7	11.8	47.2	6.1	0.6	8.5	0.4	8.9	–	0.1	–	T	0.1	–	–	–	99.5	47	15.7	1	2.75	GD	834P	
98	8530	1,191,800	884,050	1,825	21.9	7.7	48.1	10.3	0.9	7.7	1.5	9.2	–	0.2	–	0.3	1.2	–	0.2	T	100.0	42?	21.2	1	2.81	GD	1154P	
99	1177	1,196,300	883,800	1,850	24.6	5.8	50.6	8.4	–	10.3	T	10.3	–	T	–	T	0.3	–	–	–	100.0	44	19.0	1	2.78	GD	453R	

No.	1. FIELD NUMBER	COORDINATES (2) 2. X	3. Y	4. Z	5. QUARTZ	6. K FELDSPAR	7. PLAGIOCLASE	8. HORNBLENDE	9. CLINOPIROXENE	10. BIOTITE	11. CHLORITE	12. BIOTITE + CHLORITE	13. ALLANITE	14. APATITE	15. CALCITE	16. EPIDOTE	17. OPAQUE	18. PREHNITE	19. SPHENE	20. ZIRCON	21. TOTAL	22. An CONTENT OF PLAGIOCLASE	23. COLOR INDEX	24. DEFORMATION (3)	25. SPECIFIC GRAVITY	26. CLASSIFICATION (4)	27. No. OF POINTS OR LENGTH OF TRAVERSE (5)	28. REMARKS
100	8139	1,162,400	883,600	1,400	24.6	15.5	50.2	4.3	–	3.9	1.3	5.2	–	0.1	–	–	0.1	–	T	T	100.0	47	9.6	1	2.74	GD	859P	
101	8020	1,172,450	883,500	2,000	23.6	25.2	34.2	11.2	T	5.5	0.1	5.6	T	0.1	–	T	T	–	0.1	T	100.0	42	16.9	0	2.71	QM	1234P	
102	7748	1,227,950	882,800	1,000	25.8	6.7	48.9	9.9	0.1	6.6	0.7	7.3	T	T	–	T	1.3	–	T	T	100.0	42	18.6	1	2.77	GD	1000P	
103	8640	1,177,950	882,650	2,175	25.3	4.3	49.6	9.8	0.8	9.7	0.4	10.1	T	T	–	T	T	–	T	0.1	100.0	37	20.7	0	2.75	QD	1052P	
104	8159	1,169,200	882,600	2,025	21.1	19.5	45.9	9.2	T	3.6	0.4	4.0	–	0.3	–	T	T	–	T	T	100.0	37	13.2	0	2.75	GD	1061P	
105	1199	1,198,900	882,100	1,600	21.4	17.8	48.6	4.5	–	6.4	0.5	6.9	–	0.1	–	–	0.6	–	0.1	–	100.0	38	12.1	1	2.67	GD	576R	Hornblende partly chloritized
106	7756	1,238,600	881,900	950	24.7	10.4	48.6	4.5	–	10.4	0.3	10.7	–	T	–	–	1.1	T	T	T	100.0	45	16.3	1	2.77	GD	1000P	
107	113	1,215,260	880,700	1,250	23.4	8.6	45.9	4.3	–	17.2	T	17.2	–	T	–	0.2	0.4	–	–	–	100.0	46	22.1	2	2.75	GD	542R	La Quiebra Tunnel (Santiago).
108	811	1,159,500	880,400	950	18.1	2.3	47.2	19.0	–	9.9	3.0	12.9	T	0.2	–	T	T	–	0.3	–	100.0	43	32.2	2	2.79	QD	631R	Weak platy flow structure.
109	1114	1,196,300	880,300	1,650	19.3	3.3	49.2	15.7	T	11.8	0.3	12.1	–	0.1	–	T	0.3	–	–	T	100.0	46	28.1	1	2.78	QD	466R	
110	1184	1,185,300	879,700	1,900	26.2	4.0	46.6	6.5	T	16.4	0.2	16.6	–	T	–	–	0.1	–	T	T	100.0	46	23.1	1	2.77	QD	621R	
111	1516	1,189,300	878,900	1,897	18.8	14.5	47.7	10.0	–	–	8.3	8.3	–	T	T	0.6	0.1	–	T	–	100.0	35	19.0	4	2.60	GD	427R	
112	679	1,165,500	878,800	1,800	27.6	0.6	38.3	20.0	T	13.4	T	13.4	–	0.1	–	T	T	–	–	T	100.0	43	33.4	1	2.80	QD	462R	
113	784	1,179,800	878,000	2,010	21.1	5.2	52.4	5.7	–	13.9	1.4	15.3	–	0.1	–	0.1	T	–	0.1	T	100.0	38	21.2	1	2.69	QD	462R	Peñol at Guatapé
114	1182	1,183,100	877,900	1,900	20.1	7.9	58.9	4.7	–	5.7	2.7	8.4	–	T	T	T	–	–	–	T	100.0	38	13.1	0	–	GD	627R	
115	1981	1,169,100	877,500	2,050	19.7	16.7	50.6	6.7	T	5.9	0.3	6.2	–	T	–	T	T	–	0.1	T	100.0	42	13.0	0	2.74	GD	533R	
116	1183	1,186,800	876,400	1,850	21.0	14.1	40.3	9.2	–	14.6	0.6	15.2	–	0.1	–	T	0.1	–	T	T	100.0	48	24.4	0	2.68	GD	578R	
117	2655	1,205,020	876,150	1,850	26.0	10.4	51.5	5.9	–	5.3	0.1	5.4	–	T	–	T	0.7	–	–	T	99.9	38	12.0	1	2.67	GD	550R	
118	81	1,222,100	875,700	1,200	23.6	5.4	43.0	19.2	–	7.2	0.5	7.7	–	0.1	–	0.2	0.8	–	–	–	100.0	44	27.9	0	2.77	GD	503R	
119	2070	1,164,100	874,100	2,050	20.1	0.2	52.7	17.4	–	9.5	0.3	9.8	–	T	–	–	T	–	–	T	100.2	36	27.2	2	2.74	QD	580R	
120	889	1,186,700	873,800	1,875	20.2	18.2	40.2	8.0	–	12.2	1.0	13.2	–	0.2	–	–	–	–	–	T	100.0	36	21.2	1	2.71	GD	534R	
121	1178	1,184,300	873,500	2,025	38.4	8.7	34.8	6.3	–	10.8	1.0	11.8	–	T	–	T	–	–	T	–	100.0	40	18.1	1	2.70	GD	531R	Peñol at Marial.
122	15	1,243,200	872,900	1,100	13.1	5.5	64.0	7.1	–	10.0	T	10.0	–	–	–	0.2	0.1	–	–	T	100.0	44	17.4	1	2.81	QD	465R	
123	106	1,215,300	872,500	1,100	12.5	8.6	63.5	7.9	–	7.1	0.2	7.3	T	T	–	0.2	T	–	–	–	100.0	42	15.4	1	2.75	GD	418R	
124	2662	1,202,180	872,460	2,160	34.3	3.6	42.7	6.6	–	11.3	1.2	12.5	T	T	–	0.3	–	–	T	T	100.0	44	19.4	1	2.73	QD	607R	
125	2657	1,205,000	872,400	1,900	27.4	5.7	51.3	8.2	–	5.2	1.7	6.9	–	T	T	0.5	T	–	T	T	100.0	38	15.6	1	2.75	QD	578R	Weak to moderate platy flow structure.
126	870	1,180,700	871,500	1,875	42.0	4.3	40.3	8.4	–	4.4	0.4	4.8	–	T	T	0.2	T	–	–	–	100.0	44	13.4	1	2.74	QD	449R	
127	82	1,241,600	870,900	1,750	17.6	6.3	52.2	15.6	–	7.6	0.3	7.9	–	0.1	0.2	0.1	–	–	–	T	100.0	48	23.6	0	2.76	GD	552R	
128	1646	1,227,700	870,900	2,050	17.6	0.8	52.2	16.8	T	10.7	0.5	11.2	–	0.1	–	T	1.3	–	T	–	100.0	46	29.3	0	2.78	QD	542R	
129	1647	1,222,100	870,700	1,900	16.0	8.8	54.6	14.5	T	3.4	1.9	5.3	–	T	–	0.6	0.2	T	–	T	100.0	44	20.6	0	2.77	GD	619R	
130	866	1,161,100	870,600	2,050	22.0	2.5	55.4	13.5	–	6.4	0.1	6.5	T	T	–	–	0.1	–	T	T	100.0	46	20.1	2	2.78	QD	473R	
131	1648	1,234,500	870,300	1,800	23.3	15.4	36.6	10.5	0.2	12.5	T	12.5	T	0.1	–	T	1.3	–	0.1	T	100.0	44	24.3	1	–	GD	645R	
132	907	1,198,900	869,900	1,825	24.3	5.0	47.4	14.2	–	8.6	0.2	8.8	–	0.1	–	–	0.2	–	T	–	100.0	44	23.2	1	2.76	QD	508R	
133	1336	1,241,300	869,700	1,750	24.2	2.0	48.5	15.5	–	5.7	3.7	9.4	T	T	–	0.2	0.2	–	T	T	100.0	44	25.3	1	2.78	QD	489R	Weak to moderate platy flow structure.
134	158	1,179,500	869,300	1,925	14.9	0.8	58.5	9.8	–	15.0	0.6	15.6	–	0.2	–	–	0.2	–	–	–	100.0	46	25.6	2	2.81	QD	506R	
135	1180	1,172,900	868,900	2,250	19.9	0.9	46.8	24.5	–	7.5	T	7.5	–	0.1	–	T	0.2	–	0.1	T	100.0	45	32.3	1	2.80	QD	530R	Weak to moderate platy flow structure.

No.	1. FIELD NUMBER	COORDINATES (2) 2. X	3. Y	4. Z	5. QUARTZ	6. K FELDSPAR	7. PLAGIOCLASE	8. HORNBLENDE	9. CLINOPYROXENE	10. BIOTITE	11. CHLORITE	12. BIOTITE + CHLORITE	13. ALLANITE	14. APATITE	15. CALCITE	16. EPIDOTE	17. OPAQUE	18. PREHNITE	19. SPHENE	20. ZIRCON	21. TOTAL	22. An CONTENT OF PLAGIOCLASE	23. COLOR INDEX	24. DEFORMATION(3)	25. SPECIFIC GRAVITY	26. CLASSIFICATION(4)	27. No. OF POINTS OR LENGTH OF TRAVERSE (5)	28. REMARKS
136	267	1,214,000	868,400	1,500	15.4	10.6	49.6	16.6	–	6.8	T	6.8	T	T	–	0.1	0.7	–	–	T	99.8	50	24.2	1	2.70	GD	337R	
137	1285	1,171,500	868,300	2,175	25.0	T	49.5	15.5	–	9.9	T	9.9	–	T	–	T	0.1	–	T	T	100.0	44	25.5	2	–	QD	574R	
138	782	1,179,400	867,500	2,000	20.1	2.2	53.2	11.8	0.2	10.8	1.2	12.0	–	0.2	T	0.2	0.1	–	–	T	100.0	44	24.1	1	2.78	QD	435R	
139	322	1,208,300	867,300	1,200	22.0	T	52.2	15.7	T	9.6	T	9.6	T	0.1	T	0.2	0.2	–	T	–	100.0	44	25.7	1	2.78	QD	528R	
140	1599	1,250,500	866,700	1,650	18.6	2.0	57.1	15.5	–	0.3	5.9	6.2	–	0.2	–	0.5	–	–	–	–	100.1	44	22.2	1	2.75	QD	527R	
141	1673	1,211,700	866,600	1,600	23.2	7.3	48.1	13.2	–	7.6	0.2	7.8	–	T	–	0.2	0.2	–	T	T	100.0	44	21.4	1	2.76	GD	635R	
142	1793	1,245,600	866,500	1,900	32.0	32.1	25.1	6.9	–	3.3	0.3	3.6	–	0.1	–	T	T	–	–	T	99.8	35	10.5	0	2.68	QM	578R	
143	863	1,168,300	866,300	2,100	23.4	–	43.0	17.2	T	16.0	T	16.0	–	T	–	–	0.2	–	0.2	–	100.0	46	33.5	2	2.79	QD	515R	
144	1607	1,206,500	865,800	1,275	20.3	0.2	45.5	11.9	–	21.5	0.1	21.6	–	0.2	–	T	0.3	–	T	T	100.0	42	33.8	1	2.74	QD	494R	
145	1610	1,247,400	865,300	1,800	20.6	9.4	46.6	11.3	T	2.8	8.7	11.5	–	0.1	–	0.2	0.3	–	T	–	100.0	42	23.3	2	–	GD	587R	
146	879	1,190,700	864,200	2,250	26.8	5.5	47.0	5.1	–	11.2	4.3	15.5	–	T	–	T	0.1	–	T	T	100.0	42	20.7	1	2.73	GD	500R	
147	2685	1,171,100	864,200	2,100	25.1	7.0	45.6	12.4	–	9.9	T	9.9	–	T	–	–	T	–	T	T	100.0	44	22.3	3	2.78	GD	627R	
148	102	1,262,900	864,100	1,550	17.0	1.3	55.5	20.5	–	3.8	1.8	5.6	–	T	–	0.2	0.1	–	T	T	100.2	44	26.4	1	2.78	QD	461R	
149	1665	1,209,300	863,300	2,050	25.1	9.5	38.6	14.3	T	12.3	T	12.3	T	0.2	T	–	–	–	–	T	100.0	46	26.6	1	2.77	GD	567R	Gneissic
150	77	1,248,300	863,000	1,950	25.8	0.2	56.7	6.1	–	10.6	T	10.6	–	T	0.1	0.2	0.3	–	–	–	100.0	44	17.2	2	2.73	QD	575R	
151	104	1,256,900	862,700	1,550	21.2	4.9	55.1	1.0	–	17.0	0.5	17.5	–	T	0.2	–	0.1	–	T	–	100.0	40	18.6	1	2.74	QD	611R	
152	220	1,194,900	862,500	2,100	22.3	1.1	44.4	9.6	0.9	21.6	T	21.6	–	0.1	–	–	–	–	T	T	100.0	46	32.1	2	2.77	QD	517R	Strong platy flow structure.
153	893	1,203,100	862,000	1,350	25.6	11.8	33.9	18.2	–	9.7	0.1	9.8	–	T	–	–	0.3	–	0.4	T	100.0	44	28.7	2	2.75	GD	632R	
154	836	1,161,900	862,000	2,225	24.3	0.6	45.5	11.0	–	18.3	0.2	18.5	–	0.1	–	T	–	–	T	T	100.0	48	29.5	2	2.77	QD	633R	About 250 m from contact.
155	1671	1,218,000	861,900	2,200	18.1	4.7	48.0	19.3	–	–	9.6	9.6	T	T	0.3	T	–	–	T	–	100.0	45	28.9	4	2.73	QD	552R	
156	1630	1,243,100	861,500	1,950	31.0	3.5	45.0	9.3	–	9.6	0.7	10.3	–	0.2	–	0.3	0.2	–	–	T	99.8	44	20.1	0	2.71	QD	616R	
157	2684	1,174,100	861,400	2,090	22.0	T	47.2	14.4	–	15.0	1.1	16.1	–	0.1	–	0.2	T	–	T	T	100.0	48	30.6	2	2.79	QD	625R	
158	68	1,254,500	861,300	1,750	25.7	12.8	45.3	3.4	0.1	11.0	1.0	12.0	–	T	0.3	0.4	T	–	–	T	100.0	43	15.9	1	2.73	GD	551R	Hornblende partly replaced by epidote.
159	2667	1,197,350	861,100	2,200	36.3	26.3	25.8	1.7	–	9.6	T	9.6	T	T	–	0.3	T	–	–	T	100.0	38	11.6	1	2.66	QM	554 R	
160	746	1,188,500	860,900	2,300	28.6	–	54.9	7.5	–	8.9	T	8.9	T	0.1	–	–	T	–	–	T	100.0	42	16.4	1	2.74	QD	626R	
161	689	1,184,100	859,500	2,100	22.7	0.6	53.3	13.4	–	9.2	0.1	9.3	–	0.2	–	0.3	0.2	–	–	–	100.0	48	23.2	1	2.78	QD	380R	
162	5411	1,240,700	858,480	2,100	26.1	4.2	49.1	9.4	–	7.1	3.1	10.2	T	T	–	0.6	0.4	–	–	T	100.0	44	20.6	1	–	QD	421R	
163	5407	1,249,060	857,940	1,950	34.9	7.0	49.8	2.5	–	4.7	1.0	5.7	–	T	–	0.1	T	–	–	T	100.0	42	8.2	3	–	GD	538R	Muscovite, T
164	1678	1,225,300	857,700	2,400	26.1	0.7	46.8	11.8	–	12.0	2.4	14.4	–	T	–	0.2	T	–	T	T	100.0	42	26.4	3	2.77	QD	520R	Moderate platy flow structure.
165	2666	1,197,200	857,000	2,180	27.3	9.0	41.6	1.0	–	–	19.9	19.9	–	0.1	0.6	0.5	–	–	–	–	100.0	42	21.4	3	2.71	GD	629R	Chlorite: 17.7 from biotite; 2.2 from hornblende.
166	2683	1,176,600	856,100	2,087	22.4	–	59.0	13.5	–	3.6	1.0	4.6	–	0.3	–	–	0.2	–	–	–	100.0	45	18.3	4	2.78	QD	546R	
167	2663	1,194,300	856,000	2,240	35.6	7.0	39.4	8.2	–	8.7	1.0	9.7	T	T	–	0.1	T	–	–	T	100.0	40	18.0	1	2.73	GD	571R	
168	1657	1,210,500	855,900	2,300	22.0	2.2	51.0	15.6	–	8.8	0.3	9.1	–	T	–	T	0.1	–	T	T	100.0	48	24.8	1	2.80	QD	609R	Weak platy flow structure.
169	239	1,188,300	855,700	2,350	26.0	0.2	49.3	13.8	T	10.3	T	10.3	–	0.2	–	T	T	–	0.2	T	100.0	42	24.3	1	2.66	QD	457R	
170	891	1,197,700	855,200	2,250	19.2	3.5	49.5	10.2	–	17.5	T	17.5	T	T	–	0.1	T	–	–	–	100.0	42	27.8	3	2.72	QD	489R	
171	1667	1,220,600	854,300	2,500	17.4	0.2	53.8	19.7	–	7.4	0.9	8.3	–	T	–	0.4	0.2	–	–	T	100.0	45	28.6	1	2.82	QD	487R	
172	1713	1,235,500	854,200	2,550	28.2	5.7	52.7	5.9	–	7.4	0.1	7.5	–	T	–	T	T	–	–	T	100.0	40	13.4	3	2.73	QD	465R	
173	80	1,210,900	854,100	2,200	21.0	0.2	32.8	27.7	T	17.1	0.3	17.4	–	T	–	0.2	0.2	–	0.1	T	100.0	46	45.6	2	2.82	QD	584R	Weak platy flow structure.

No.	1. FIELD NUMBER	COORDINATES (2) X 2.	COORDINATES (2) Y 3.	COORDINATES (2) Z 4.	5. QUARTZ	6. K FELDSPAR	7. PLAGIOCLASE	8. HORNBLENDE	9. CLINOPYROXENE	10. BIOTITE	11. CHLORITE	12. BIOTITE + CHLORITE	13. ALLANITE	14. APATITE	15. CALCITE	16. EPIDOTE	17. OPAQUE	18. PREHNITE	19. SPHENE	20. ZIRCON	21. TOTAL	22. An CONTENT OF PLAGIOCLASE	23. COLOR INDEX	24. DEFORMATION (3)	25. SPECIFIC GRAVITY	26. CLASSIFICATION (4)	27. No. OF POINTS OR LENGTH OF TRAVERSE (5)	28. REMARKS
174	1301	1,217,200	853,100	2,350	26.0	6.9	47.5	11.5	T	7.6	0.2	7.8	T	0.2	–	T	T	–	0.1	T	100.0	48	19.4	3	2.79	GD	497R	Moderate platy flow structure.
175	686	1,180,300	852,500	2,100	19.3	–	48.4	17.2	–	14.0	0.3	14.3	–	0.2	–	–	0.4	–	–	–	99.8	44	31.9	3	2.78	QD	506R	
176	2687	1,201,220	852,440	1,350	24.8	2.7	49.2	5.6	–	16.3	0.2	16.5	–	0.1	–	0.7	T	–	–	T	99.6	45	22.1	4	2.76	QD	618R	Average of several analyses.
177	85	1,260,800	851,800	2,125	34.5	2.6	51.5	6.7	–	2.9	0.7	3.6	–	T	0.1	1.0	0.1	–	–	–	100.1	46	10.5	1	2.76	QD	481R	
178	5403	1,242,580	851,580	2,500	33.2	9.1	48.9	3.3	–	5.3	0.2	5.5	–	T	–	T	–	–	T	T	100.0	44	8.8	1	– –	GD	579R	
179	973	1,204,700	851,500	2,400	27.2	0.4	43.7	10.3	T	18.2	0.1	18.3	T	0.1	–	T	T	–	–	T	100.0	44	28.6	1	2.79	QD	601R	Moderate platy flow structure.
180	3	1,210,700	851,100	1,150	21.5	0.9	52.3	5.8	–	19.2	T	19.2	–	0.1	–	–	0.2	–	T	T	100.0	44	25.2	1	2.73	QD	514R	
181	2669	1,206,570	850,650	2,400	22.8	0.5	43.8	16.9	–	15.8	T	15.8	T	0.1	–	–	0.1	–	T	T	100.0	48	32.8	4	2.78	QD	587R	Weak platy flow structure.
182	JL-61	1,252,700	848,740	2,500	28.4	1.5	52.5	0.1	–	17.1	0.2	17.3	T	T	–	0.2	–	–	–	T	100.0	48	17.4	2	2.68	QD	606R	
183	1686	1,224,900	848,500	2,500	22.6	11.1	43.0	7.3	–	15.2	0.5	15.7	–	0.2	–	T	0.1	–	T	T	100.0	45	23.1	2	2.75	GD	584R	K feldespar is microcline.
184	5043	1,261,200	848,360	2,200	25.4	0.1	47.3	9.2	–	16.1	1.6	17.7	–	0.3	–	–	T	–	T	T	100.0	49	26.9	1	–	QD	593R	
185	2671	1,204,460	848,120	2,350	23.8	4.2	52.5	7.0	–	10.6	1.6	12.2	–	0.1	–	0.2	T	–	–	T	100.0	48	19.4	1	2.75	QD	624R	
186	275	1,187,500	848,100	2,150	25.6	6.1	50.3	10.0	–	7.8	T	7.8	–	0.2	–	T	T	–	0.1	T	100.1	40	17.9	2	2.68	GD	615R	
187	1684	1,244,100	847,900	2,600	32.6	3.0	53.8	5.1	–	4.9	0.6	5.5	–	T	–	T	–	–	–	T	100.0	44	10.6	2	2.77	QD	549R	
188	JL-63	1,250,900	847,300	2,650	27.1	1.4	56.5	5.2	–	8.9	0.3	9.2	T	0.1	–	0.5	–	–	–	–	100.0	42	14.4	2	2.72	QD	605R	
189	750	1,265,000	846,800	2,530	23.0	0.4	50.6	11.0	–	13.9	1.0	14.9	–	0.1	–	T	T	–	–	T	100.0	47	25.9	1	2.78	QD	567R	
190	83	1,229,700	846,700	2,550	26.0	13.1	43.3	6.1	T	11.4	T	11.4	–	T	–	T	0.1	–	T	T	100.0	46	17.6	2	2.74	GD	650R	
191	2670	1,208,640	846,560	2,300	20.2	10.0	43.1	14.6	–	10.9	0.7	11.6	–	0.1	–	–	0.4	–	–	T	100.0	45	26.6	1	2.75	GD	631R	
192	2675	1,222,500	846,200	2,450	28.4	2.7	42.8	6.2	–	19.4	0.2	19.6	–	0.1	–	0.2	T	–	–	–	100.0	42	26.0	1	2.74	QD	608R	
193	1587	1,238,900	844,400	2,700	27.8	4.5	46.5	9.0	–	12.0	T	12.0	–	0.1	–	0.1	–	–	T	T	100.0	42	21.1	3	2.76	QD	600R	
194	395	1,242,400	844,300	2,750	23.0	10.4	43.0	10.2	–	13.1	0.2	13.3	T	T	–	0.1	–	–	T	T	100.0	43	23.6	2	2.73	GD	559R	
195	1693	1,215,700	844,300	2,300	30.2	0.2	51.3	8.4	–	9.8	T	9.8	–	T	–	T	0.1	–	–	T	100.0	42	18.3	2	2.75	QD	488R	
196	1588	1,238,900	843,300	2,750	25.4	3.1	46.2	12.8	–	11.6	0.2	11.8	–	0.2	–	0.5	T	–	T	T	100.0	48	25.1	3	2.76	QD	515R	Weak platy flow structure; K feldespar is microcline.
197	1894	1,219,700	841,500	2,350	34.4	3.3	51.0	1.1	–	9.8	0.3	10.1	–	T	–	0.1	T	–	–	T	100.0	40	11.3	3	2.65	QD	620R	
198	99	1,263,600	841,400	1,965	22.8	10.7	45.0	5.6	–	15.6	0.3	15.9	–	T	–	–	–	–	–	T	100.0	44	21.5	2	–	GD	421R	
199	2677	1,233,400	840,300	2,550	20.5	–	46.3	15.4	–	14.5	T	14.5	–	0.3	–	–	3.0	–	–	–	100.0	48	32.9	1	2.83	QD	630R	Calcic cores (An_{62}) in plagioclase.
200	2	1,215,300	840,100	2,350	21.8	4.4	48.2	12.4	–	13.0	0.1	13.1	T	T	–	0.1	T	–	–	T	100.0	46	25.6	2	2.75	QD	628R	Peñol at Entrerríos.
201	4	1,211,400	839,100	2,200	31.4	1.6	45.5	8.7	–	12.4	0.1	12.5	–	0.1	–	–	–	–	0.2	T	100.0	40	21.4	3	2.74	QD	480R	Moderately strong platy flow structure.
202	2678	1,231,400	837,940	2,450	20.2	5.3	50.0	13.2	T	10.9	0.3	11.2	T	0.1	–	T	T	–	–	T	100.0	46	24.4	1	2.78	QD	579R	
203	1532	1,246,900	837,900	2,700	21.4	0.1	51.6	8.7	–	17.6	0.2	17.8	T	0.1	–	0.3	T	–	–	T	100.0	46	26.8	1	2.79	QD	548R	
204	1589	1,241,500	837,900	2,750	23.2	0.6	52.5	8.8	–	14.4	0.1	14.5	–	0.3	T	0.1	T	–	–	T	100.0	44	23.4	2	2.77	QD	610R	
205	1717	1,236,500	837,400	2,650	22.6	0.6	49.8	21.0	–	5.4	0.1	5.5	–	T	–	0.4	0.1	–	T	–	100.0	42	27.0	3	2.75	QD	613R	
206	1592	1,242,400	837,000	2,700	37.2	0.5	48.5	1.7	–	10.7	0.6	11.3	–	0.2	–	0.6	–	–	–	T	100.0	44	13.6	2	2.71	QD	568R	K feldespar is microcline.
207	1533	1,249,500	835,200	2,750	21.8	6.0	50.2	9.5	–	11.9	0.3	12.2	–	0.1	–	0.2	–	–	–	T	100.0	46	21.9	2	2.75	GD	579R	
208	2469	1,233,500	830,700	1,700	15.1	3.7	39.2	22.8	–	17.0	0.4	17.4	–	0.5	–	0.2	1.1	–	–	T	100.0	45	41.5	3	2.74	QD	500R	Coarse-grained; muscovite, T
209	1534	1,251,700	830,100	2,650	28.0	6.1	49.0	5.3	–	11.4	0.1	11.5	–	T	–	0.1	–	–	–	T	100.0	44	16.9	2	2.75	GD	549R	

No.	1. Field number	Coordinates (2) 2. X	3. Y	4. Z	5. Quartz	6. K feldspar	7. Plagioclase	8. Hornblende	9. Clinopyroxene	10. Biotite	11. Chlorite	12. Biotite + chlorite	13. Allanite	14. Apatite	15. Calcite	16. Epidote	17. Opaque	18. Prehnite	19. Sphene	20. Zircon	21. Total	22. An content of plagioclase	23. Color index	24. Deformation (3)	25. Specific gravity	26. Classification (4)	27. No. of points or length of traverse (5)	28. Remarks
210	1837	1,235,500	828,800	2,600	22.5	2,3	55.2	5.7	–	13.9	0.2	14.1	–	T	–	0.1	0.1	–	–	T	100.0	44	20.0	2	2.69	QD	617R	
211	RAA-21	1,249,420	825,200	2,700	15.8	–	61.2	10.5	–	11.9	0.5	12.4	–	T	–	T	0.1	–	–	–	100.0	40	23.0	2		QD	563R	
212	583	1,253,500	825,000	2,450	22.3	3.3	46.2	15.8	–	11.8	T	11.8	–	0.1	–	0.5	T	–	T	T	100.0	44	28.1	1	2.77	QD	591R	Weak to moderate platy flow structure.
213	1538	1,255,100	824,900	2,000	19.6	1.9	40.0	9.4	–	28.8	T	28.8	–	0.3	–	T	T	–	–	T	100.0	48	38.2	3	2.78	QD	615R	Moderate platy flow structure; muscovite, T
214	1820	1,245,100	822,900	2,800	21,8	1,4	50,5	14,5	–	10.4	0.4	10.8	T	0.2	–	0.8	T	–	T	T	100.0	40	26.1	3	2.76	QD	621R	
Average					23.9	6.7	48.4	9.3	0.1	9.3	1.6	10.9	T	0.1	0.1	0.2	0.2	T	0.1	T	100.0	43.5	20.9	1.3	2.76	QD		
Maximum values					42.0	32.1	68.7	27.7	1.7	28.8	22.4	28.8	0.2	0.5	6.5	2.0	3.0	0.2	1.7	0.1		55	45.6	4	2.80			
Minimum values					12,5	0.0	25.3	0.0	0.0	0.0	0.0	1.6	0.0	T	0.0	0.0	0.0	0.0	0.0	0.0		33?	7.5	0	2.65			
Standard deviation					4.62	5.74	6.28	5.07	0.28	5.07	3.01	4.28	0.03	0.10	0.51	0.32	0.37	0.02	0.19	0.03		4.38	6.46		0.04			

1. Samples 2 through 2687 are in the petrographic collection of the Facultad Nacional de Minas, Medellín; samples 5043 through 8681 and JL-61, JL-63, and RAA-21 are in storage, INGEOMINAS, Dirección Regional, Medellín.
2. Colombian coordinate system with X and Y each equal to 1,000,000 at Bogotá; distance in meters north of the latitude of Bogotá is (X -1,000,000); distance in meters west of the longitude of Bogotá is (1,000,000-Y); Z is elevation in meters above sea level.
3. See text for explanation.
4. QD, quartz diorite; GD, granadiorite; QM, quartz monzonite (O'Connor, 1965).
5. R indicates Rosiwalanalysis, figure is length of traverse in millimeters; P indicates point count analysis, figure is number of points.
6. T, trace.

TABLE 4.

CHEMICAL ANALYSIS OF TWO SAMPLES OF THE NORMAL FACIES, ANTIOQUIAN BATHOLITH[1]

		1	;2
Fiel number		8526	8527
USGS laboratory number		W168–911	W168–912
	X	1,207,150	1,209,900
Coordinates	Y	908,900	908,200
	Z	925	1,000
SiO_2		63.6 %	62.5 %
TiO_2		0.41	0.58
Al_2O_3		16.2	15.2
Fe_2O_3		1.9	1.7
FeO		3.0	4.0
MnO		0.15	0.38
MgO		2.6	4.2
CaO		6.2	6.6
Na_2O		3.2	2.8
K_2O		2.0	1.3
P_2O_5		0.12	0.27
H_2O^-		0.20	0.22
H_2O^+		0.38	0.34
CO_2		0.06	0.05
Total		100.0 %	100.1 %

1. Chemical analysis by rapid rock analysis methods , U.S. Geological Survey, Washington, D.C., See Table 3 for modal analysis of these samples.

Untwinned potassium feldspar occurs as anhedral grains chiefly in optically continuous domains that interstitially fill spaces between euhedral grains of plagioclase, biotite, and hornblende (Fig. 6). These domains achieve surprisingly large sizes; commonly they cover more than a square centimeter, and in some cases, am entire thin section. Most contacts with plagioclase and quartz are smooth (Fig. 6); embayments or other evidence of corrosion or resorption by potasium feldspar normaly are wanting. Microperthite is weakly developed in some samples. The potassium feldspar is everywhere fresh, even in samples of otherwise extensively altered rock.

Hornblende is chiefly isubhedral in fresh to euhedral prisms, although in a few samples it has the unusual habit of an interstitial mineral (Fig. 7). Pleochroism is normally X = light yellow tan; Y = medium green; Z = medium brownish green with $X < Y < Z$.- Moderate to strong dispersion with $r > v$ is prevalent. Electron microprobe analyses of hornblende in five samples of granodiorite (Table 5) show them to have rather uniform compositions that correspond closely to those of hornblendes from igneous rocks of similar compositions quoted by Deer, Howie, and Zussman (1963, p. 277-281). Hornblendes in a few samples has orange-brown Y and Z colors. One of these hornblendes is among those analyzed (Table 4, col. 3). Excluding slightly higher TiO_2, its composition differs little from its companion hornblendes with green Y and Z colors. The low total of the analysis of the orange-brown hornblende, however, could reflect a relatively higher Fe_2O_3 : FeO ratio.

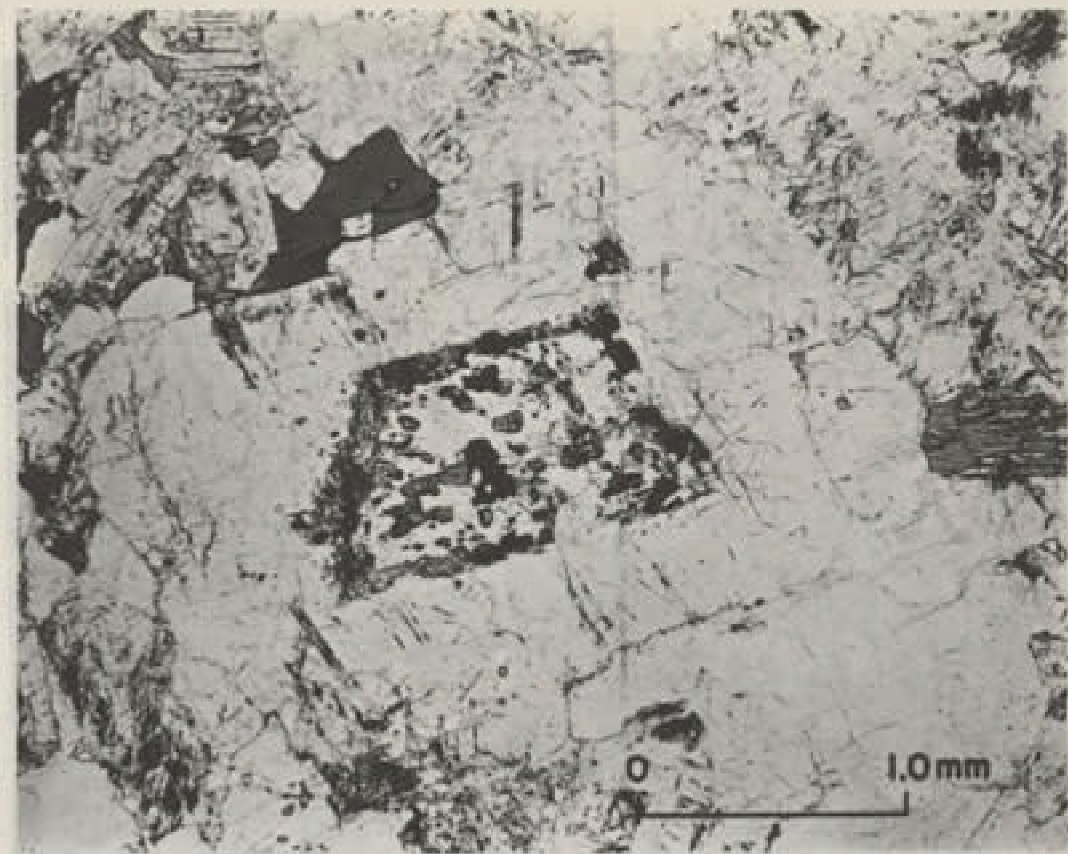

FIGURE 4. Inclusions of clinopyroxene, clinopyroxene rimmed with hornblende, and hornblende in core of plagioclase crystal. Sample 8538.

FIGURE 5. Optically continuous interstitial quartz. Sample 7515.

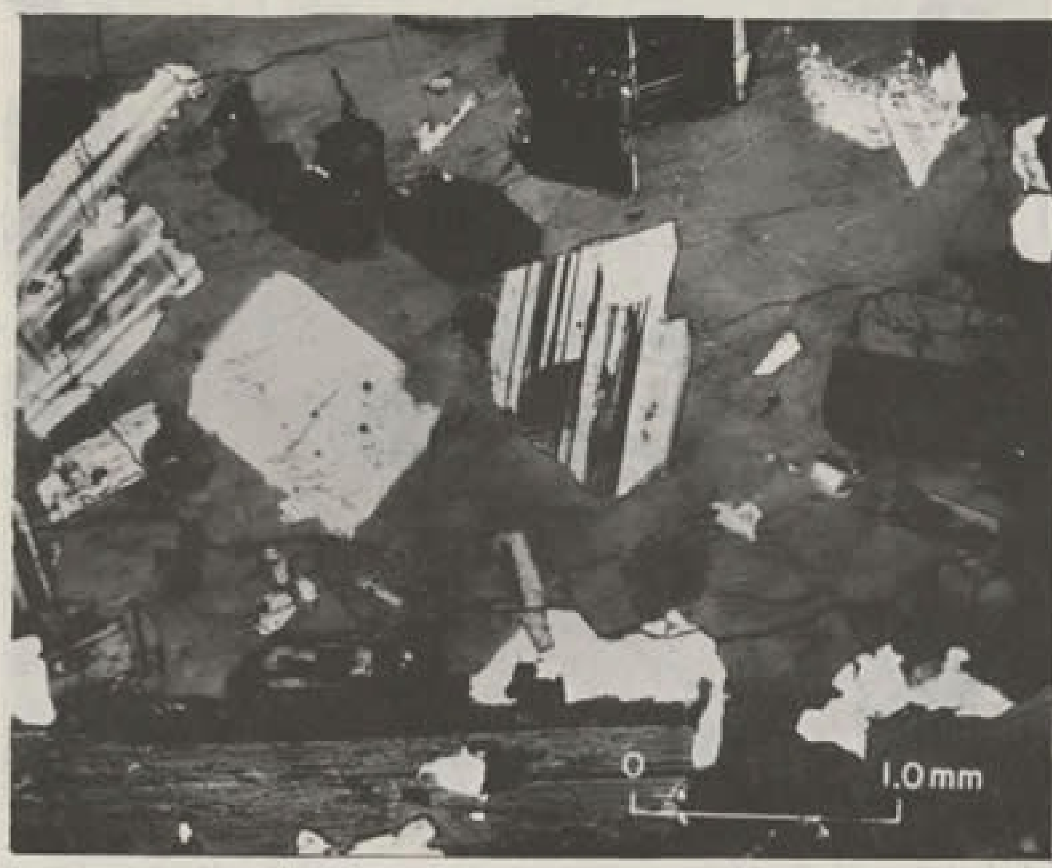

FIGURE 6. Large field of optically continuous interstitial potassium feldspar. Sample 7523.

Ragged cores of colorless clinopyroxene occur in some grains of hornblende. An especially large one is shown in Figure 8. In a few samples, the only clinopiroxene present has been preserved as tiny inclusions in the cores of plagioclase crystals (Fig. 4). More common than the occurrence of clinopyroxene, however, is the occurrence of hornblendes with bleached cores that contain tiny vermicular inclusions of quartz (Fig. 9). The bleached cores were produced by the conversion of preexisting clinopyroxene cores to amphibole, a reaction that liberates quartz. Similar complex hornblendes from tonalite in the Cornucopia stock, Oregón, have been figured by Taubeneck (1967, pl. 1).

Biotite forms subhedral to euhedral boocks that in more than two thirds of the samples studied are free of deformation. Pleochroism is strong with X = light yellow; Y = Z = deep golden brown. Biotite coexistent with the less common orange-brown hornblende, however, has a different pleochroism; X = light yellow brown. Y = Z = medium red brown. Generally a part of the biotite in each thin section, mostly between 5 and 10 percent, has been altered to bright green chlorite (Fig. 9). The biotite is far less resistant to chloritization than coexisting hornblende; even in samples where chloritization of biotite is complete, neighboring hornblende grains are preserved unaffected. Biotites in about half the samples of the normal facies contain a colorless to pale yelow alteration product with moderately high relief and low birefringerence in slim concordant lenses which have bowed apart the (001) cleavage. A similar alteration of biotite, interpreted as deuteric, has been described from parts of the Boulder Creek batholith, Colorado, by Wrucke (1965), who found the lenses there to be composed of prehnite and hydrogarnet (?). (The prehnite noted in the modal analysis (Table 3) is in interstitial grains amongst the felsic minerals and is not spatially related to biotite alteration).

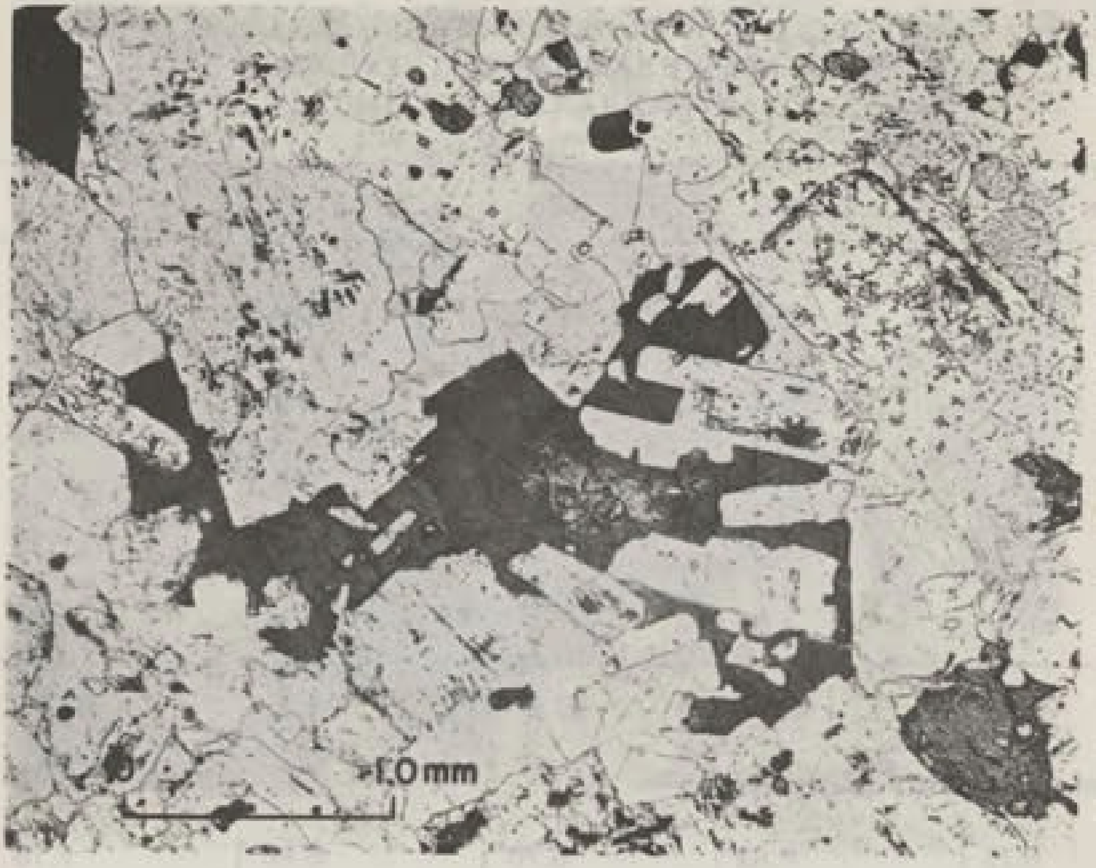

FIGURE 7. Anhedral interstitial hornblende with core of clinopyroxene. Sample 7544.

Ubiquitous accessory minerals of the normal facies are apatite, magnetite, and zircon. Others, in order of decreasing abundance, are sphene, epidote, pyrite, calcite, allanite and prehnite. Apatite is particularly abundant and constitutes more than 0.1 percent of most samples. Large grains are anhedral or subhedral, whereas grains less than 0.1 mm are sharply euhedral. Zircon forms subhedral to euhedral clear prisms. Those in biotite are characteristically unaccompanied by radiohalos.

7.3.2. MAFIC CLOTS

Fine-grained, massive, dark gray mafic clots, commonly with megacrysts of plagioclase or hornblende 2 to 5 mm long, are irregularly distributed in the normal facies over much of the batholith in disregard of both nearness and nature of surrounding rocks. The clots, known to Antioquian geologists as **gabarros**, are spherical, lenslike, or more commonly spindle-shaped bodies with maximum dimensions mostly between 5 and 50 cm (Fig. 10). Although proportionately enriched in mafics, gabarros are composed of the same minerals, except quartz, as the enclosing rock of the normal facies. A modal analysis of a typical gabarro from east of Amalfi showed it to be composed of plagioclase (An_{39}) 38 percent, potassium feldspar 25 percent, biotite 24 percent, hornblende 13 percent, and accessory minerals.

7.3.3. FELSIC FACIES

Five bodies of rock constituting a felsic facies have been mapped within the east half of the batholith (Fig. 3). The combined area of these bodies is 203 km^2 (78 mi^2), or

TABLE 5.

ANHYDROUS ELECTRON MICROPROBE ANALYSES OF AMPHIBOLES IN FIVE SAMPLES OF THE NORMAL FACIES. ANTIOQUIAN BATHOLITH[1]

Sample	1534	2670	2685	7992	7997
SiO_2	45.0	45.6	44.7	46.0	49.0
TiO_2	1.5	1.1	1.9	1.1	0.7
Al_2O_3	8.8	8.3	8.9	7.8	5.8
FeO*	20.7	19.0	16.9	18.3	16.6
MnO	0.5	0.4	0.3	0.4	0.3
MgO	9.4	10.8	11.2	11.5	13.4
CaO	11.5	11.3	11.9	11.6	11.3
Na_2O	1.0	1.2	1.0	1.0	1.0
K_2O	1.0	1.0	1.1	1.0	0.6
Total	99.4	98.7	97.9	98.7	98.7

Number of ion based on 23 oxygens:

Ion	1534	Sum	2670	Sum	2685	Sum	7992	Sum	7997	Sum
Si	6.75	8.00	6.82	8.00	6.70	8.00	6.86	8.00	7.18	8.00
Aliv	1.25		1.18		1.30		1.14		0.82	
Alvi	0.30	5.00	0.28	5.00	0.27	5.00	0.23	5.00	0.18	5.00
Ti	0.17		0.12		0.21		0.12		0.08	
Mg	2.09		2.41		2.50		2.56		2.93	
Fe	2.44		2.19		2.02		2.09		1.81	
Fe	0.16	2.07	0.19	2.05	0.10	2.05	0.19	2.09	0.22	2.04
Mn	0.06		0.05		0.04		0.05		0.04	
Ca	1.85		1.81		1.91		1.85		1.78	
Na	0.29	0.48	0.35	0.54	0.29	0.50	0.29	0.48	0.28	0.39
K	0.19		0.19		0.21		0.19		0.11	

1. Analyses by T. Feininger at the Department of Mineral Sciences, Smithsonian Institution, Washington, D.C., U.S.A. See Table 2 for modal analyses of these rocks.

* Total iron reported as FeO.
Following the IMA nomenclature of amphiboles (LEAKE, 1978), 1534 is ferro-hornblende; 2670 and 2685 are are edenite; and 7992 and 7997 are magnesio-hornblende.

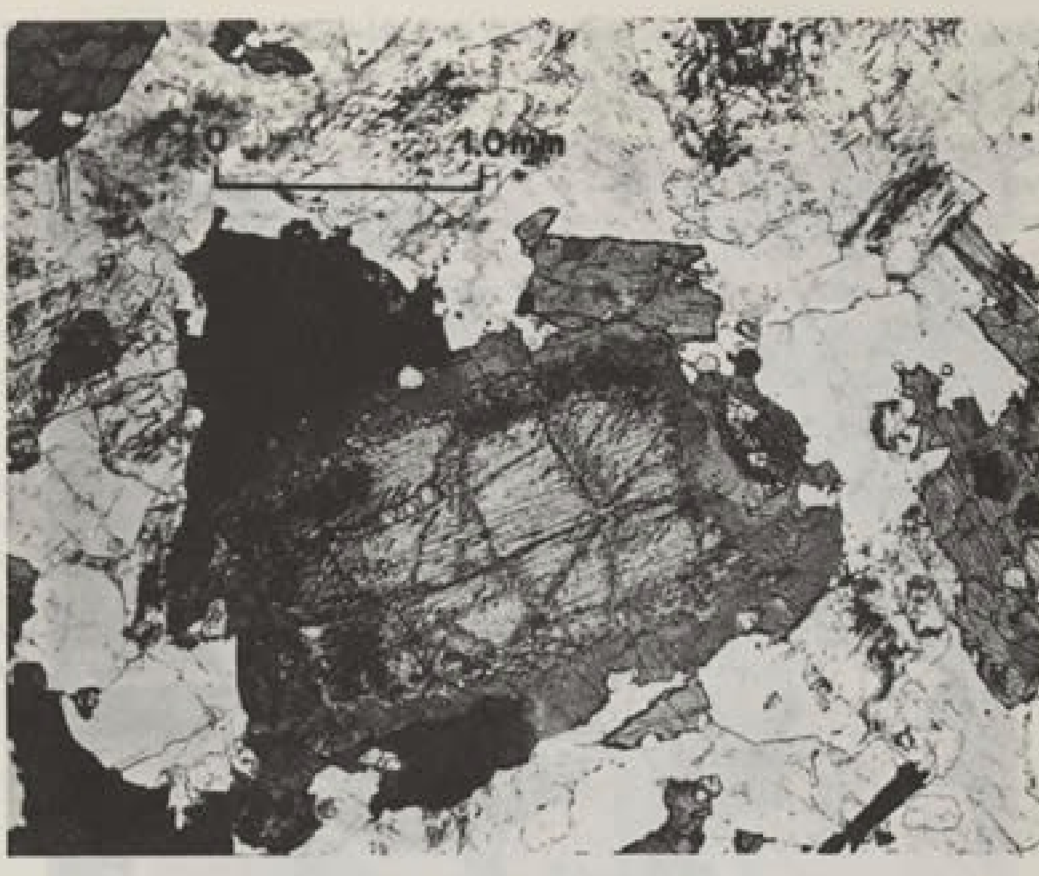

FIGURE 8. Large core of clinopyroxene in hornblende with an incomplete rim of biotite. Sample 8012.

FIGURE 9. Two subhedral crystals of hornblende with bleached cores containing tiny inclusions of vermicular quartz. Note partially chloritized biotite. Sample 7811.

FIGURE 10. Gabarros in the normal facies of the Antioquian batholith, Río Guatapé downstream from Balseadero.

about 2.8 percent of the whole batholith. Exposures of the felsic facies are largely restricted to residual boulders. These are especially plentiful on the hills west northwest of Yalí, atop the high mountains nearly midway between Amalfi and Yolombó, and along the roads from Santo Domingo to the Río Nare and from Maceo to La Susana. The contact between the felsic and normal facies is nowhere exposed. It is interpreted as gradational, but it is also possible that the felsic facies occurs as myriadas of discrete small bodies because in some places residual boulders of the two rock types are intimately mixed. Recent test drilling by Cristalería Peldar Ltda. between Alejandría and Santo Domingo revealed that rock of the felsic facies there is inhomogeneous and locally grades into more mafic rock whose modal composition falls within the field of the normal facies (Table 6).

The felsic facies is chiefly light tan or beige, massive medium-to coarse grained, hypidiomorphic to xenomorphic, leucocratic granodiorite or quartz monzonite. Part of this facies is porphyritic with subhedral to euhedral phenocrysts of quartz as much as 1 cm long. The phenocrysts are particularly conspicuous on residual boulders where they weather into relief and give the rock a pimply surface. With advanced weathering the large quartzes are freed and become concentrated as a grus in the soils. This is especially well developed along the road from Maceo to La Susana. The felsic facies is less resistant to weathering than the normal facies and truly fresh rock is rare.

TABLE 6

MODAL ANALYSIS OF THE FELSIC FACIES, ANTIOQUIAN BATHOLITH

	Test boring No. 1. Depth 30 m	Test boring No. 2. Depth 33 m
Quartz	35.8	29.5
K. feldspar	24.7	11.9
Plagioclase	36.4	49.0
Hornblende	—	2.6
Biotite	2.0	3.1
Chlorite	0.6	0.5
Apatite	Tr.	0.2
Opaques	0.5	0.9
Sphene	Tr	0.2
Zircon	Tr.	Tr.
Hydrogarnet	—	Tr.
Number of points	2,136	2,384
Specific gravity	2.65	2.65
Color index	3.1	7.3
An. content	32.	34.

Coordinates; X = 1,200,800; Y = 8,881,620

Samples from the Santo Domingo - Alejandría road at the Nare river.

Modal analysis of eight samples of the felsic facies are given inTable 7. Compared to the normal facies, the felsic facies is richer in quartz and potassium feldspar, has a more sodic plagioclase, a much lower color index, and consequently a lesser specific gravity.

TABLE 7

MODAL ANALYSIS AND AVERAGE COMPOSITION OF EIGHT SAMPLES OF THE FELSIC FACIES, ANTIOQUIAN BATHOLITH[1]

	1.	2.	3.	4.	5.	6.	7.	8.	9.
Fiel number	7549	7615	7645	7729	7730	7751	7946	8393	Average of felsic facies
Coordinates X	1,232,050	1,216,200	1,216,200	1,214,700	1,232,600	1,236,300	1,181,450	1,201,350	
Coordinates Y	908,150	926,000	926,000	925,050	908,650	892,500	897,975	882,500	
Coordinates Z	1,350	825	825	850	1,600	1,650	1,300	1,575	
Quartz	35.9	38.6	37.0	26.4	33.6	33.2	42.4	30.8	34.7
K feldspar	25.9	22.3	23.9	22.0	30.8	14.2	6.1	20.0	20.7
Plagioclase	36.5	33.3	31.9	41.6	33.2	45.1	44.8	44.5	38.9
Biotite	1.6	3.1	4.6	5.0	2.2	5.2	6.2	3.9	4.0
Chlorite	—	—	—	—	0.2	1.6	0.3	0.5	0.3
Muscovite	—	2.4	2.6	5.0	—	—	—	—	1.3
Allanite	—	—	—	—	—	—	T	—	
Apatite	—	—	—	—	—	T	T	T	
Epidote	T	—	—	—	—	0.4	T	—	
Garnet	—	0,2	T	T	—	—	—	—	
Opaque	0.1	—	—	—	T	0.2	0.2	0.2	0.1
Sphene	—	—	—	—	—	T	—	—	
Zircon	—	T	T	T	T	0.1	T	0.1	
Total	100.0	99.0	100.0	100.0	100.0	100.0	100.0	100.0	100.0
An content of plagioclase	28	—	23	23	27	36	28	35	29
Color index	1.7	3.3	4.6	5.0	2.4	7.4	6.7	4.6	4.5
Specific gravity	2.65	2.64	2.65	2.64	2.62	2.65	2.67	2.64	2.65
Classification	QM	QM	QM	GD	QM	GD	GD	GD	
Number of points	1,138P	1,192P	1,000P	500P	500P	1,000P	1,255P	1,230P	

1. Values in volume percent. Analyst: T. Feininger.

Under the microscope quartz is unstrained. Non-phenocrystic grains are anhedral. Plagioclase is mostly oligoclase, though it ranges to sodic andesine in some samples. Grains are zoned and twinning is more subdued than in the andesine of the normal facies. Grain margins in contact with potassium feldspar are commonly myrmekitic. Potassium feldspar forms anhedral compact grains rather than the interstitial fill characteristic of the normal facies. Grains are microperthitic and exhibit weak grid twinning. Some have incomplete thin rims of albite. The mafic mineral is exclusively biotite, in part chloritized. Absortion is weaker than that in biotite of the normal facies, with X = pale straw yellow to colorless, and Y = Z = medium brownish green. Included zircons are surrounded by strong pleochroic halos. The accessory mineral suite of the felsic facies is impoverished (Table 7), although the pair granet and muscovite, unknown in the normal facies, occurs with frequency.

7.3.4. GABBROIC FACIES

Seven small bodies of gabbroic rock with an aggregate area of 15 km^2 (only 0,2 percent of the batholith) have been mapped on the east half of the Antioquian batholith. The largest body (5.5 km^2) of the gabbroic facies is between San José on the Antioquian Railroad and the site of Cristales. Nowhere were rooted outcrops found; the outline of each body was mapped exclusively on the occurrence of residual boulders. The boulders are exceptionally abundant and particularly conspicuous owing to their rust-stained and deeply pitted surfaces; at first glance they resemble iron meteorites. In may places creep has carried the boulders far from their point of origin so that the size of probably all the bodies (Fig. 3) is exaggerated.

Fresh rock of the gabbroid facies is black to dark green or dark brown, coarse to medium grained, and hypidiomorphic to idiomorphic. Mostly it is equigranular, although some samples carry poikilitic phenocrysts of black hornblende as much as 5 cm long. The composition of the gabbroic facies is higly variable; it ranges from pyroxenite to hornblende gabbro. The most ultramafic samples are perfectly fresh in thin section. Many of the other samples are altered, showing saussuritic plagioclase, pale green fibrous amphibole pseudomorphic after pyroxene, and the partial to complete alteration of olivine to "iddingsite" and talc. Modal analysis of eight samples and chemical analysis of two samples of gabbroic facies rocks are given in tables 8 and 9 respectively.

Although the contact between the gabbroic and normal facies is not exposed, the petrography of the residual boulders indicates that it must be gradational. For example, on the body between San José and Cristales are found boulders of pyroxenite nearly free of feldespar (Table 8, col. 1), boulders of mafic gabbro (Table 8, col. 2) and boulders of hornblende gabbro with a little quartz (Table 8, col. 3). Other boulders, not represented in Table 8, stepwise bridge the gap between hornblende gabbro and typical quartz diorite of the batholith's dominant normal facies. The only ultramafic rock is found in this body.

7.3.5. CONSANGUINOUS STOCKS

Surrounding the Antioquian batholith are numerous stocks of a variety of igneous rocks (Fig. 3). Most of the stocks are petrographically so unlike the batholith that a genetic relationship between them and the batholith can be easily discarde. Nevertheless, several, several sotocks are composed of rock indistinguishable from that of the normal facies o f the batholith. These petrographically uniform stocks have a total area of 322 km^2 (124 mi^2) and are considered consanguinous with the Antioquian batholith (Table 10).

TABLE 8

MODAL ANALYSIS OF EIGHT SAMPLES OF THE GABBROIC FACIES, ANTIOQUIAN BATHOLITH[1]

		1.	2.	3.	4.	5.	6.	7.	8.
Field number		7633	7634	7636	7706	7743	7744	7754	7944
Coordinates	X	1,209,200	1,207,650	1,207,750	1,240,450	1,238,000	1,242,500	1,240,600	1,192,300
	Y	910,700	913,500	913,600	923,550	899,000	900,200	923,950	901,050
	Z	1,050	1,150	1,100	1,025	1,575	1,275	1,075	1,050
Quartz		—	—	T	9.2	0.3	—	0.6	—
K feldspar		—	—	—	0.2	—	—	1.7	—
Plagioclase		5.8	21.4	66.4	49.6	23.0	51.8	25.3	72.9
Olivine		0.3	11.9	—	—	—	—	0.6	0.9
Orthopyroxene		54.3	20.2	—	—	2.4	—	—	—
Clinopyroxene		27.6	20.4	0.1	—	1.2	11.5	20.0	10.3
Amphibole		11.0	25.7	26.1	29.1	67.7	30.5	50.4	10.2
Biotite		T	T	—	2.9	—	—	0.1	—
Chlorite		—	—	2.1	6.6	0.9	3.9	0.4	—
Apatite		—	—	—	0.3	T	0.1	0.2	—
Calcite		0.2	T	0.3	0.1	—	—	0.3	T
Epidote		—	—	4.1	—	0.4	0.9	—	2.3
"Iddingsite"		—	T	—	—	3.2	0.5	0.2	3.4
Opaque		0.8	0.1	0.9	1.1	0.6	0.8	0.1	T
Sphene		—	—	T	0.9	—	—	0.1	—
Spinel		—	0.3	—	—	—	T	—	T
Talc		—	—	—	—	0.3	—	—	—
Total		100.0	100.0	100.0	100.0	100.0	100.0	100.0	100.0
An content of plagioclase		88	80	70	60	89	73	70	70
Color index		94.0	78.3	33.3	40.6	76.7	48.1	71.9	27.1
Specific gravity		3.29	3.13	2.93	2.88	3.02	2.94	3.05	2.90
Number of points		1,000P	1,000P	766P	950P	1,000P	1,000P	1,000P	1,170P

1 Values in volume percent - Analyst: T. Feininger.

TABLE 9

CHEMICAL ANALYSIS OF TWO SAMPLES OF THE GABBROIC FACIES, ANTIOQUIAN BATHOLITH[1]

		1.	2.
Field number		7633	7634
USGS laboratory number		W168-916	W168-917
Coordinates	X	1,209,200	1,207,650
	Y	910,700	913,500
	Z	1,050	1,150
SiO_2		52.1 %	46.1 %
TiO_2		0.39	0.29
Al_2O_3		5.6	12.2
Fe_2O_3		1.4	1.8
FeO		11.4	8.8
MnO		0.09	0.02
MgO		21.3	17.8
CaO		6.4	10.3
Na_2O		0.32	0.96
K_2O		0.08	0.18
P_2O_5		0.04	0.02
H_2O-		0.17	0.17
H_2O+		0.63	1.00
Total		99.9 %	99.6%

1. Chemical analysis by rapid rock analysis methods, U.S. Geological Survey, Washington, D.C. See Table 8 for modal analysis of these samples.

TABLE 10.

MODAL ANALYSIS AND AVERAGE COMPOSITION OF FOUR SAMPLES CONSANGUINOUS STOCKS OF THE ANTIOQUIAN BATHOLITH[1]

		1.	2.	3.	4.	5.	6.
Field number		7507	7814	60	1642		Average normal facies (Table 3)
Coordinates	X	1,202,300	1,248,200	1,191,300	1,226,300	Average	
	Y	924,400	928,000	831,900	821,500		
	Z	725	725	2,325	2,600		
Quartz		23.2	32.7	27.6	20.6	26.0	23.9
K feldspar		4.3	6.9	0.6	0.3	3.0	6.7
Plagioclase		62.9	49.1	55.1	51.2	54.6	48.4
Hornblende		0.6	0.8	4.4	14.2	5.0	9.3
Biotite		6.1	9.9	10.2	12.1	9.6	9.3
Chlorite		1.3	0.3	1.4	1.0	1.0	1.6
Allanite		—	—	T	—		
Apatite		0.3	0.1	T	0.1		
Epidote		T	T	0.7	—		
Opaque		1.1	—	—	0.5		
Sphene		0.2	0.2	T	—		
Zircon		—	0.1	T	T		
Total		100.0	100.1	100.0	100.0		
An content of plagioclase		33	39	44	44	40	43.5
Color index		9.3	11.2	16.7	27.8	16.3	20.9
Specific gravity		2.70	2.70	—	—		
Classification		QD	QD	QD	QD		
Analysis		1,000P	1,764P	480R	415R		

1. Values in in volume percent. Analysts: G. Botero A., and T. Feininger.

7.3.6. DIKES

The ensuing discussion will deal with two distinct groups of dikes: apophysy dikes of batholith rocks in surrounding prebatholith rocks, and postbatholith dikes that cut the batholith itself.

Apophysy dikes of the Antioquian batholith in host rocks are infrequent although the apparent scarcity may in part be an artifact enhanced by paucity of outcrop. Dikes in noncalcareous rocks differ little from the normal facies of the batholith beyond having a somewhat finer grain size. Some small dikes far removed from the batholith contact have a curious spotted appearance imparted by dark spherical aggregates 5 mm in diameter composed of fibrous amphibole. The compositions of dikes in calcareous rocks, however, depart widely from the composition of the batholith. These dikes are medium to fine grained, massive and hypidiomorphic equigranular. Superficially, except for their darker color, they resemble the dikes in noncalcareous rocks, but closer inspection shows they are greatly depleted in quartz and commonly contain 25 percent or more clinopyroxene (Table 11). Presumably the incoming magma that crystallized to form these dikes was desilicated by

TABLE 11.
MODAL ANALYSIS OF SIX SAMPLES FROM DIKES OF THE ANTIOQUIAN BATHOLITH IN CALCAREOUS ROCKS[1]

		1.	2.	3.	4.	5.	6.
Field number		7628	7687	7699	7735	7747	8157
	X	1,215,650	1,251,500	1,248,800	1,252,050	1,242,300	1.162.250
Coordinates	Y	917.625	903,000	896,150	902,500	911,300	918,650
	Z	950	1,350	1,500	1,400	1,275	425
Quartz		0.1	10.2	0.4	9.9	3.2	—
K feldspar		—	20.4	1.3	11.9	1.2	0.2
Plagioclase		72.0	41.0	60.4	—	56.9	54.0
Orthopyroxene		17.2	—	—	—	—	—
Clinopyroxene		—	25.0	32.3	65.2	35.0	—
Amphibole		7.8	—	3.2	—	—	42.1
Biotite		0.8	—	—	—	—	—
Chlorite		0.3	—	0.1	—	0.2	1.2
Apatite		T	—	—	0.4	T	0.6
Calcite		—	0.8	0.7	—	0.2	0.6
Epidote		—	0.5	0.1	9.0	0.3	—
Opaque		1.8	—	0.4	0.2	T	1.1
Prehnite		—	—	T	—	—	—
Scapolite		—	0.5	—	—	—	—
Sphene		—	1.6	1.1	3.4	3.0	0.2
Zircon		—	—	—	—	—	T
Total		100.0	100.0	100.0	100.0	100.0	100.0
An content of plagioclase		64	38	50	—	46	48
Color index		27.9	27.1	37.2	77.8	38.5	44.6
Specific gravity		2.89	2.90	2.94	3.22	2.96	2.89
Number of points		769P	939P	1,108P	1,000P	1,000P	1,711P

1. Values in volume percent. Analyst: T. Feininger.

the enclosing calcareous rocks, mostly marble, but including also calcite - bearing quarzite and gneiss. This view is supported by the common development of wollastonite, diopside, vesuvianite, or tremolite in marble adjacent to the dikes, each attesting to the introduction of silica.

The Antioquian batholith is cut by innumerable dikes with knife-sharp contacts that range in composition from andesite to felsite and alaskite. Owing to scarcity of outcrop, the presence of most of the dikes is indicated only by cobbles and small boulders of these rocks left behind upon the decomposition of the less resistant enclosing batholith rock.

By far the most abundant are dark gray or gray-green, very fine grained to aphatitic, porphyritic dikes of intermediate composition from 2 cm to 1 m thick. Phenocrysts are euhedra of black hornblende or white plagioclase from 1 to 5 mm across. Near contacts the long axes of phenocrysts are aligned parallel to dike walls and their matrix is aphanitic. Many of the dikes are multiple with successive intrusions exhibiting chilled borders against earlier ones.

The grain of the thin intermediate dikes is too fine to allow modal analysis and petrographic classification. However, rock in the chilled margins of an exceptional dike 800 m thick, 5 km west of Cisneros (Tab. 12), is identical to rock of the thin intermediate dikes and the compositions of the large dike is therefore probably much like that of its innumerable finergrained companions.

TABLE 12.

MODAL ANALYSIS OF A SAMPLE FROM THE INTERIOR OF THE LARGE INTERMEDIATE DIKE 5 KM WEST OF CISNEROS[1]

		1.
Field number		7503
	X	1,215,150
Coordinates	Y	882,750
	Z	1,725
Quartz		15.4
K. feldspar		4.3
Plagioclase		62.7
Clinopyroxene		0.9
Hornblende		8.4
Biotite		7.0
Chlorite		0.4
Apatite		0.1
Epidote		T
Opaque		0.8
Total		100.0
An content of plagioclase		40
Color index		17.5
Specific gravity		2.78
Classification		QD
Number of points		1.000P

1 Values in volume percent. Analyst: T. Feininger.

A modal analysis of a sample from the interior of the large dike (Table 12) shows it to be a quartz diorite somewhat poorer in quartz and richer in plagioclase, but otherwise not unlike the normal facies of the Antioquian batholith.

Based on this evidence, the prevalent dark gray intermediate dikes are held to be chiefly dacite and andesite.

In outcrop the thin intermediate dikes commonly exhibit curved and even amoeboid contacts (Fig. 11). This suggests that although the batholith had fully crystallized before intrusion of the dike magma, it was still hot enough to yield somewhat plastically.

Dikes of rocks with other compositions are much less common. Medium grained, bright pink alaskite was exposed in tunnels during construction of the Nare underground hydroelectric development, 8 km west of San Rafael. East of the same town are found a few thin dikes of pink pegmatite with accessory black tourmaline. Pink to beige saccharoidal aplite occurs near the southern tip of the batholith, south of San Luis. It is composed of one third quartz, one third potassium feldespar, one third sodic plagioclase, and traces of muscovite and chloritized biotite. Dikes of aphanitic pink felsite (rhyolite?) mostly less than 10 cm thick, occur sparsely throughout the batholith.

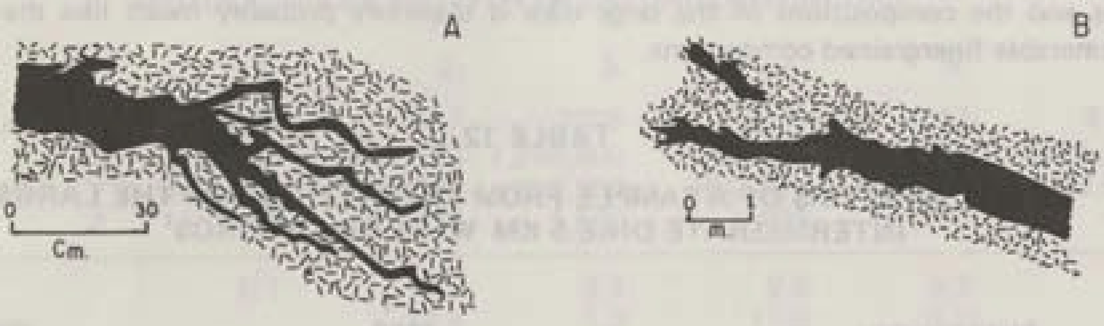

FIGURE 11. Fine-grained intermediate dikes in the normal facies of the Antioquian batholith and a consanguinous stock. A: Quebrada Cantayús, height 1000 m, 5 km east of Cisneros. B: Río Nus, 1 km upriver from Caracolí. T. Feininger field sketches.

8. REGIONAL VARIATIONS

We have emphasized the general uniformity of the normal facies throughout the Antioquian batholith. Unifortunately, due to paucity of outcrop, neither the density nor the assurance of impartiality of our sampling are sufficient to allow a computer-run analysis of regional variations of the composition or other properties of the broadly homogeneous Antioquian batholith. Nevertheless, our long familiarity with this body of rock allows us to make a few general observations. The only systematic variations we have found are from east to west; north-to-south variations appear random. To illustrate east-to-west variations, we have arbitrarily divided the batholith into five north-south tiers, bounded by the following lines of longitude: Y = 910,000; 887,500; 865,000 and 842,500. Analyzing samples confined to thesese tiers, potassium feldspar shows a general increase from west to east, whereas both color index and degree of deformation show steady decreases (Table 13). Other parameters show less systematic or random changes.

The arresting development of interstitial potassium feldspar (Fig. 6) is common only in the eastern half of the batholith. To the west, concomitant with lessening abundance, potassium feldspar is increasingly limited to subequant anhedral or isolated intertitial wedges. The steady increase of color index from east to west is due chiefly to increases of total hornblende and biotite. Increases of these minerals individually are erratic.

A qualitative measure of the degree of deformation to which each sample of the normal facies has been subjected was recorded on a scale of 0 to 4 (Table 3). Divisions are as follows: 0, no evidence of deformation; 1, undulatory extinction of quartz; 2, bending of biotite; 3, bending of plagioclase; 4, cataclasis. In many samples annealing must have followed deformation. For example, samples with bent biotite but unstrained quartz are relatively common. In table 13 the degree of deformation of the normal facies in each of the north south tiers is the simple average of the degree of deformation recorded for corresponding individual samples. The progressive increase of this parameter from east to west is striking. Of the 90 samples from the eastmost two tiers, 32, or more than one third, show no evidence of deformation. On the other hand, of the 69 samples from the westmost two tiers, only one is underformed.

One other parameter, grain size, subjectively appears to us to increase subtly from east to west. However, lacking systematic measurements, we cannot substantiate this observation quantitatively.

TABLE 13.

REGIONAL VARIATIONS IN THE ANTIOQUIAN BATHOLITH

	1	2	3	4	5	6
Coordinates	933,500 to 910,000	910,000 to 887,500	887,500 to 865,000	865,000 to 842,500	842,500 to 820,000	Average normal facies
Number of samples	29	61	55	51	18	214
Modal K feldspar	7.6	8.0	7.9	4.4	2.9	6.7
Color index	18.9	19.1	21.2	22.3	24.6	20.9
Degree of deformation	0.85	0.87	1.05	1.89	2.11	1.3
	East	----------	----------	----------	West	

9. STRUCTURAL GEOLOGY

Study of the structural geology of the Antioquian batholith is impeded by the scarcity of outcrops of fresh rock. Nevertheless, enough observations can be made on the sparce outcrops on the myriads of residual boulders, and on the virtually endless exposures of rotted rock along mule trails to piece together a coherent picture.

9.1. FLOW STRUCTURE

Nearly all the Antioquian batholith is composed of rock perfectly isotropic even to the practiced eye. This statement is supported by the frequency with which the long axes or planar surfaces of gabarros fail to have common orientations even in large outcrops. Neither rock near contacts, nor in the consaguinous satellite stocks is any less massive than that in the interior of the batholith.

Planar flow structure (foliation), however, is visible in some isolated or small groups of residual boulders. The foliation is imparted by parallel arrangement of biotite books, hornblende prisms or platy grains of plagioclase, and is mostly weakly developed. In only one exposure, a residual boulder 1.8 km southwest of the junction of the road to Cristales with the main road, were two divergent flow structures seen. Here, feebly foliated quartz diorite is truncated nearly at right angles by slighltly more strongly foliated but otherwise identical quartz diorite. Foliation in the second rock parallels its contact with the first rock. Excluding their weak foliations, both rocks are typical representatives of the normal facies of the batholith. Also, in some outcrops parallel alinement of the long axes of gabarros imports a linear flow structure.

A particularly outstanding example can be seen on the east face of the Guatapé peñol. In most places this parallelism is vague and enclosing batholith rock ramains massive. The bearing of this linear flow structure ranges widely, but its plunge is uniformly gentle, mostly subhorizontal, and only rarely does it exceed 30 degrees.

9.2. CONTACTS AND INCLUSIONS

The contact of the Antioquian batholith must approach a sharp nearly smooth surface judging by the virtual absence of apophysy dikes, or other mechanical mixing with adjacent enclosing rocks. In only three places was the actual contact found exposed and in each it is razor sharp. Sketches of parts of each exposure are given in Figure 12. In two of the three exposures the batholith rock is massive to within less than 5 cm of the contact, and in the third it is massive throughout. Only where emplaced in amphibolite is the batholith contact diffuse and characterized by a zone of mixing. The zone mixing is as much as 100 m wide and consists of coarsely recrystallized amphibolite with lenses and irregular masses of quartz diorite and diorite. The mixed rock has a migmatitic or agmatitic structure. Excellent examples are exposed 1.4 km northwest of Maceo and at the north end of the consanguinous stock at Caracolí.

It is likely that virtually the entire contact of the batholith is discordant. Topographic relief is generally suffcient over the edges of the batholith to determine at least crudely the attitude of the contact. Wherever this was done, we found it to be discordant. Even where strikes of the contact and of foliation in host rocks are coincident, dips of the two differ.

Along the east edge of the batholith east of Yalí for example, foliation in host quartzite and gneiss dips steeply east or west, whereas the contact of the batholith dips gently west under the metamorphic rocks (see also Fig. 3, east half of section A-A').

Much of the batholith contact dips gently and approximates a roof rather than a wall. This relationship is best demonstrated in the northeast quarter where local relief at the edge batholith exceeds 500 m and the attitude of the contact can be mapped with precision (Fig. 3, section C-C'). The gentle dip of the roof, at least over the northern half of the batho-

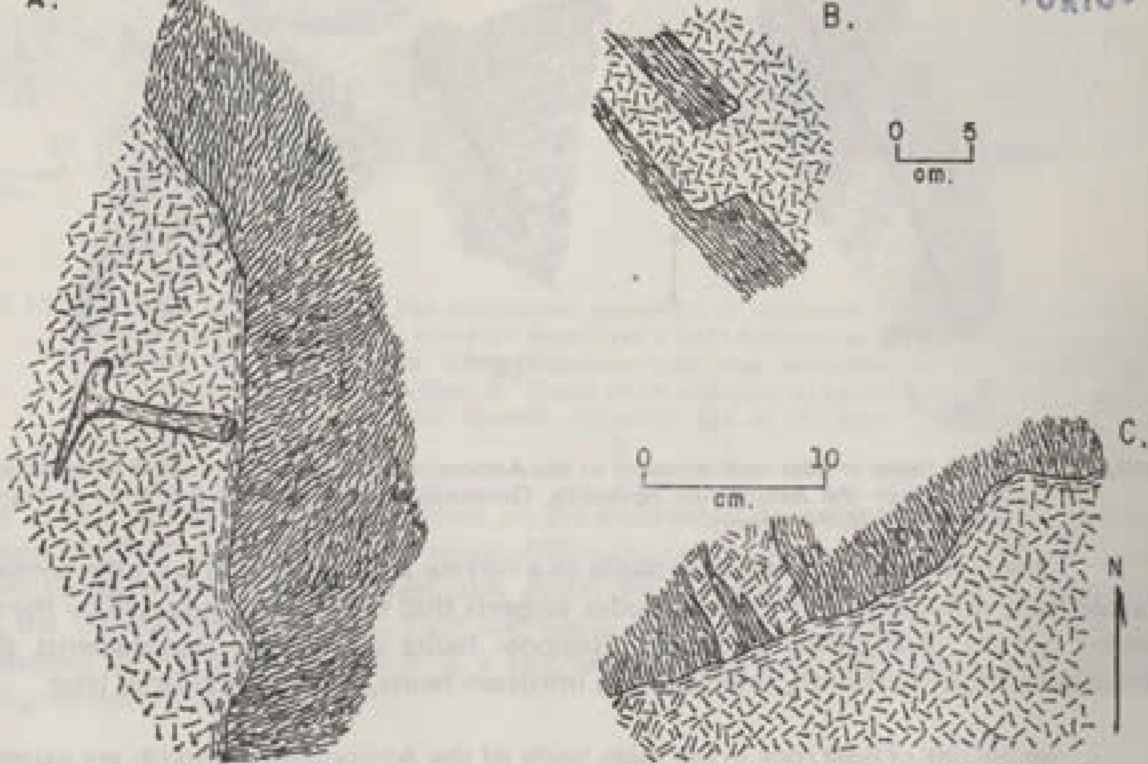

FIGURE 12. Contacts of the Antioquian batholith. A: Contact with feldspathic aluminous gneiss. Tributary of the Santa Bárbara gorge, 5 km notheast of Balsadero. B: Contact with hornblendic, laminated skarn, Quebrada Santo Tomás. C: Contact of a large dike (or of the main batholith body ?) and migmatitic feldspathic gneiss, Quebrada Bélgica. Field sketches by T. Feininger.

lith, is further substantiaded by the progressive and uniform decrease in elevation of the contact at a rate of from 20 to 30 meters per kilometer from west to east. At Yarumal the contact is at 2400 m. Sixty kilometers to the east, near Amalfi, it is at 1600 m. Near El Tigre, 30 km further east, it is at 1000 m, and 15 km east of the longitude of El Tigre, east of Maceo, the contact has descended to only 600 m. Elsewhere, particularly in the western half of the batholith, we have studied the contact in less detail. However, there too a gentlydipping roof is consistent with field observations. Accordingly, we have shown a roof with this attitude in nearly all our cross sections (Fig. 3) and consider it a general characteristic of the Antioquian batholith. Only in the extreme southeast corner is the contact steep to vertical (Fig. 3, section E-E').

Deformation of host rocks that with confidence can be atributed to the Antioquian batholith is surprisingly restricted. Regional geologic mapping peripheral to the batholith (Fig. 3; INGEOMINAS, FEININGER and others, 1970) shows that changes in neither style nor intensity of deformation in host rocks are recognizable as the batholith is approached. True, folding of low-grade schist in the Amalfi area, not far from the batholith, is especially intense. However, structural attitudes are regionally uniform and are truncated by the batholith. Furthermore, lineations in the schist plunge into, not off the batholith, nor do they parallel the contact (Fig. 3). It is unlikely that this locally intense deformation is related to the coincidentally nearby batholith. On the other hand, high-grade gneisses host to the batholith in a belt about 100 m wide adjacent to the contact in the northeast corner are cut by numerous tiny faults with displacements up to a few centimeters (Fig. 13).

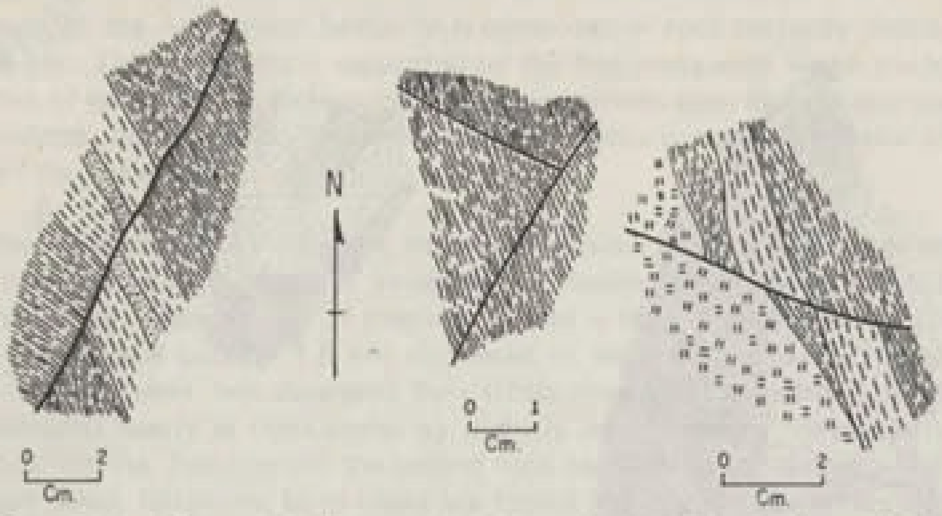

FIGURE 13. Small faults in host rock adjacent to the Antioquian batholith. Laminated feldspathic gneiss, 20 m from the Antioquian batholith. Quebrada Bélgica, 4.8 km S 9°E of El Tigre. Field sketches by T. Feininger.

The restriction of these tiny faults to a narrow zone peripheral with the contact and the apparent randomness of their attitudes suggests that they were producted by the emplacement of the neighboring batholith. Regional faults with large displacements directly attributable to the batholith, referred to as intrusion faults, will be considered later.

Inclusions of host rock in the main body of the Antioquian batholith are exceedingly uncommon and occur at only half dozen sites. At one place, a small body of intrusive breccia with clasts of fine-grained gneiss was found (Fig. 14). Inclusions in consaguinous stocks (Fig. 15) are somewhat more abundant but still are not commonplace features. All inclusions have sharp contacts with their internal structure truncated by the surrounding igneous rock.

9.3. INTRUSION FAULTS

A series of long parallel faults with northwesterly strikes occurs principally in host rocks but also in the adjacent half of the Antioquian batholith from a point 15 km north west of Yalí south to San Carlos.

A complementary set of shorter faults with northeast strikes are found between San Carlos and Caracolí (Fig. 3). Excluding the Nare, Bizcocho and Caldera faults, discussed apart later, these faults share a common feature. They are either confined chiefly to the gently-dipping roof over the batholith, or they separate batholith and roof rocks. The northwest-striking faults generally expose batholith rocks on their southwest blocks, whereas the northeast-striking faults do so on their northwest blocks. These interesting faults are here referred to as intrusion faults because of their genetic ties to the emplacement of the Antioquian batholith. They represent the grandest recognized deformation of host rocks by the batholith.

The intrusion faults were caused by differential foundering of the subhorizontal roof into magma of the Antioquian batholith during or shortly after intrusion. The foundering was stepped in a regular fashion, that is, roofrocks northwest of the northeast-striking faults foundered relative to roofrocks on the southeast, and roofrocks northeast of the northwest-

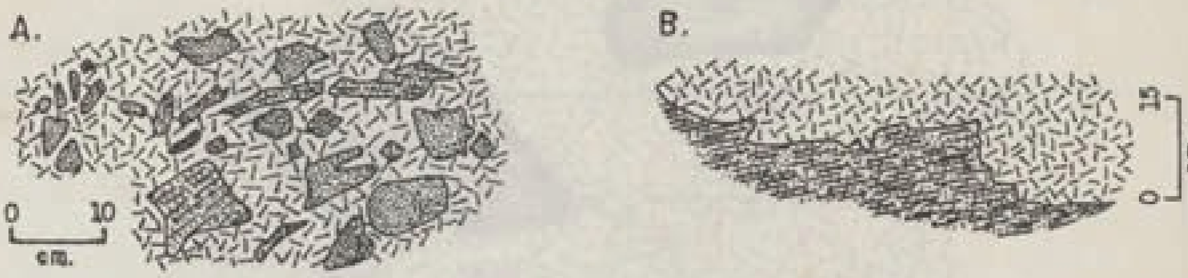

FIGURE 14. Inclusions of host rock in the Antioquian batholith. A: Intrusive breccia. Abundant inclusions of fine grained gneiss; many of them have a faint foliation and show well-defined contacts with the quartz diorite. Some inclusions have been recrystallized to a massive hornfelsic texture. Quebrada San Blas. B: Detail of an inclusion of laminated quartzitic gneiss in quartz diorite. Quebrada Peñol Grande, elevation 325 m (A, from a photograph; B, field sketch by T. Feininger).

striking faults foundered relative to those on the southwest. An exception is the east end of the Balseadero fault south of Jordán where roofrocks on the southwest sank. This fault had a scissors displacement. The sharpness with which the south-striking proboscis of batholith crosses the trace of the Balseadero fault and heads south to pass between the Cocorná sur and Palestina faults suggests that it is a thin sheet concordant with the steeply-dipping enclosing metamorphic rocks.

The origin proposed for the intrusion faults is sustained by field observations. Where the faults separate the batholith from roofrocks, the latter are throughly shattered and brecciated, whereas adjacent batholith rock dispays no deformation. This relationship is particularly well exposed at Balseadero, a small settlement at the confluence of the Ríos Guatapé and San Carlos, where cordierite gneiss in a quarry north of the road has been reduced to angular rubble with no pieces larger than a fist, while quartz diorite in outcrops across the road in the river are whole and completely undistubed. The general relationships of intrusion faults at depth can be seen at the east end of section A-A' and in section D-D' (Fig.3). A detailed interpretation of the west end of the Balseadero fault is given in Figure 16.

Projections of most of the northwest-striking intrusion faults can be followed as lineaments into the batholith on air photographs. This is particularly true of the Nare fault. Upstream from its entrance into the metamorphic host rocks, the Río Nare flows across the batholith in a singularly arresting straight canyon 300 m deep and 23 km long. The subparallel Bizcocho and Caldera faults to the southwest are similarly reflected by lineaments, though less spectacularly so. Surprinsingly, in none of the three faults does strongly sheared or brecciated rock crop out. The canyon of the Nare affords nearly continuous outcrop, but aside from locally saussuritized rock, severely deformed rock is absent. Three samples of batholith rock from the Nare fault (7965, 7969 and 7968) show only degrees of deformation on our scale of 2,1, and 0 respectively. Samples from the Bizcocho (7933 and 7937) and Caldera (8019) faults show similar or only slightly higher degrees of deformation (3 and 1, an 2, respectively).

The remarkable parallelism of the northwest-striking intrusion faults suggests that they existed as regional faults in the metamorphic rocks prior to the emplacement of the batholith. Stresses imposed by intruding magma reactivated these preexisting faults which offered long zones of weakness in the batholith's roof. It is likely that ancient drainage patterns on the roof of the batholith were forcibly readjusted to the renewed faulting. A

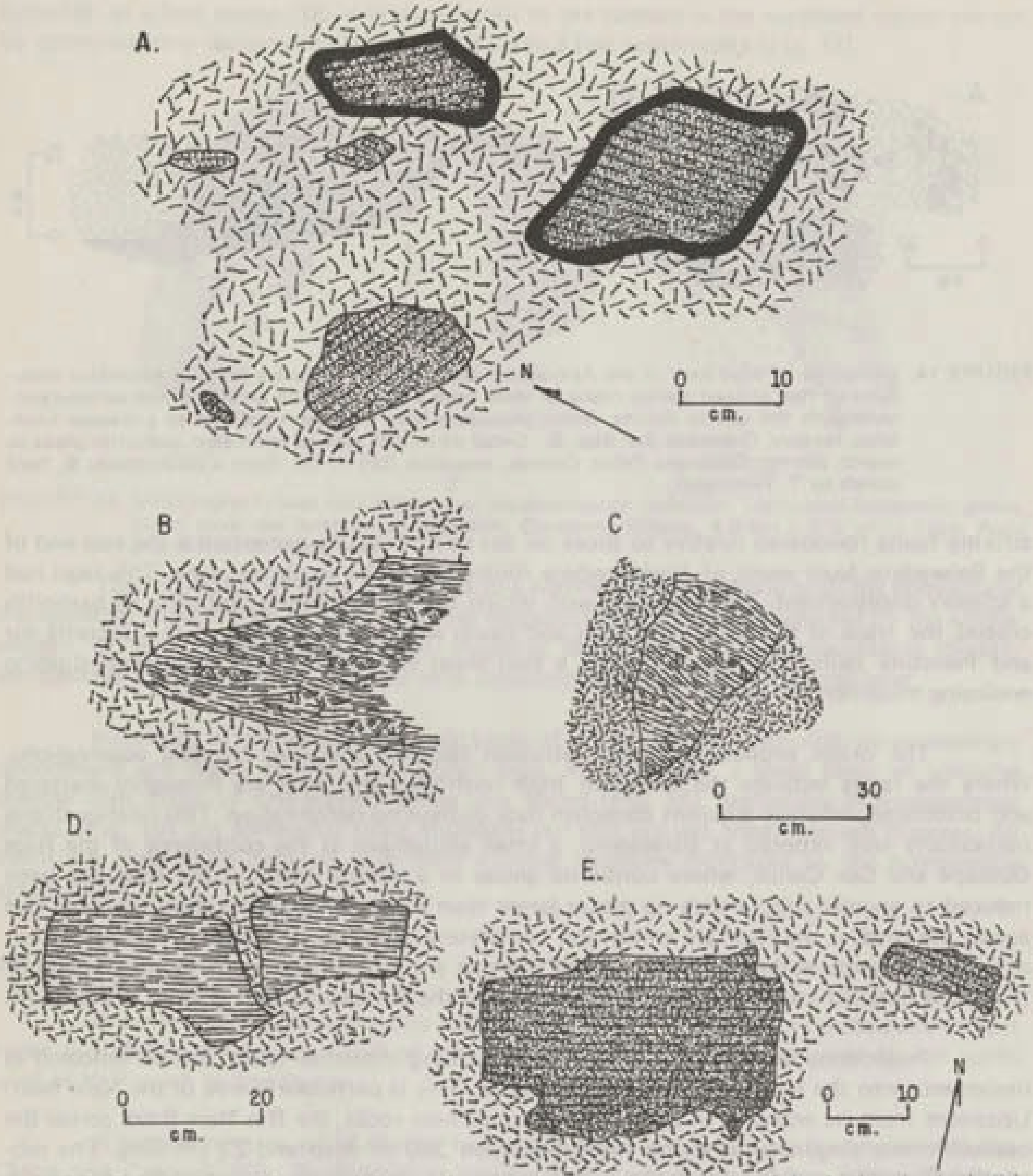

FIGURE 15. Inclusions of host rock in apophyses and consaguinous stocks of the Antioquian batholith. A: Quartzite inclusions, some with reaction borders, in an apophysis of quartz diorite. El Torito, 14 km ESE of Amalfi. B: Inclusion of feldspathic gneiss. Loose boulder, Caracolí - Santa Isabel del Nus road, 800 m from Caracolí. C: Inclusions of migmatitic gneiss. Boulder in a creek, 1 km southeast of Caracolí. D: Inclusions of quartz-feldspar-mica gneiss. Boulder, Río Mata, 5,5 km northwest of El Tigre. E: Inclusions of laminated quartzite, Quebrada Calabozo, elevation 1450 m. Field sketches by T. Feininger.

regular pattern emerged with drainage by subsequent streams that followed the more easily eroded shattered rock along the northwest-striking faults. Erosion progressively removed the roof over the batholith and bared the underlying homogeneous igneous rock. Smaller streams were able to evolve new courses unrelated to their ancestry. Some master streams such as the ancestral Nare and Guatapé, however, had cut such deep canyons that they had become prisoners of their courses. With their ancestry largely erased, these rivers, now superposed streams, continue to deepen their canyons. All this is not to say that no movement has occurred along the projections of the northwest-striking intrusion faults in the batholith.

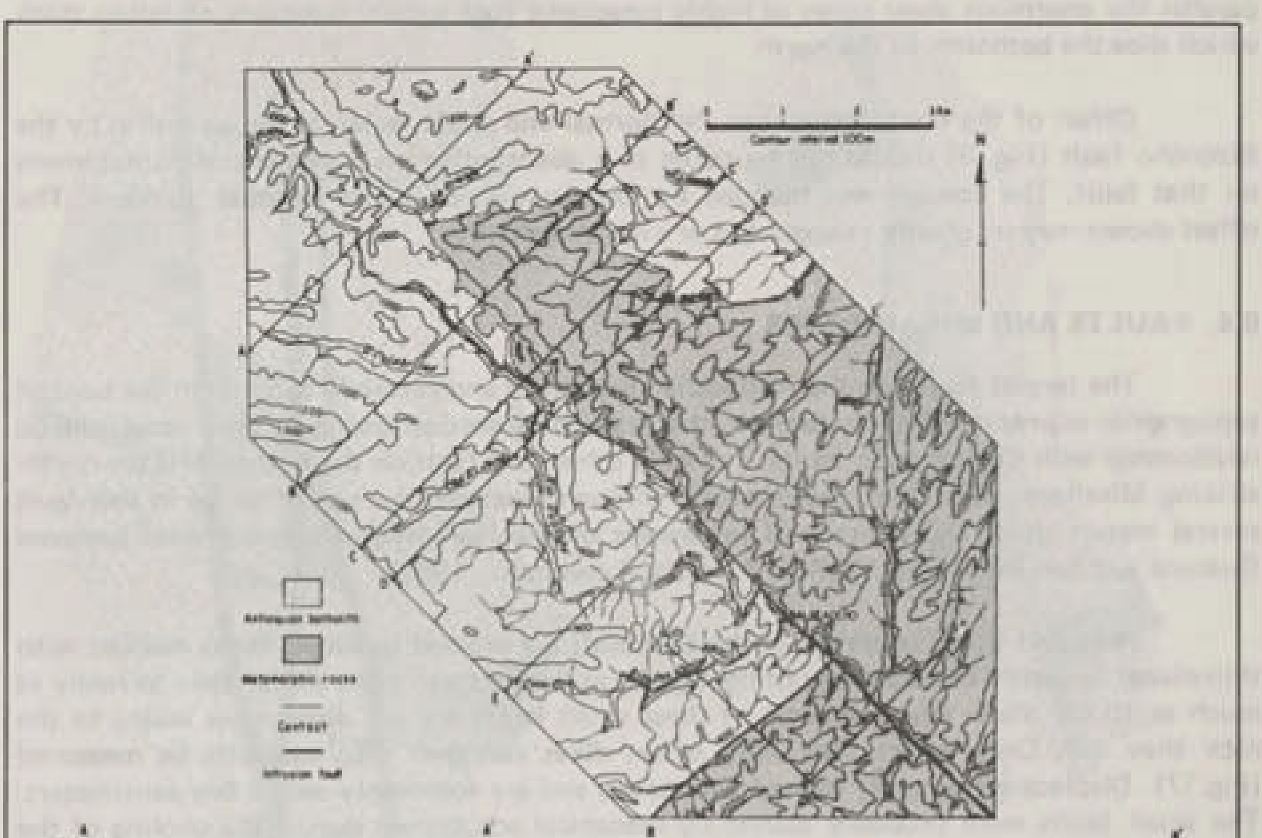

FIGURE 16. Geologic sketch map and cross section of the northwest end of the Balseadero Fault.

Some movement almost certainly has taken place which is not surprinsing in view of their proposed prebatholith history and their regional extent. Batholith rock in the canyon of the Río Nare or along the Bizcocho and Caldera faults, although not severely deformed is nevertheless more deformed than that on the adjacent mountains. Furthermore, these faults parallel the enormous shear zones of highly cataclastic rock locally hundreds of meters thick which slice the batholith to the north.

Offset of the contact between the normal and felsic facies of the batholith by the Bizcocho fault (Fig. 3) should not be taken as a quentitative measurement of displacement on that fault. The contact was mapped by examination of sparse residual boulders. The offset shown may be greatly exaggerated or even imaginary.

9.4. FAULTS AND SHEAR ZONES

The largest faults on the Antioquian batholith, and certainly those with the boldest topographic expression, were treated in the preceeding section owing to their close genetic relationship with the intrusion faults. The only other long fault on the batholith is the north-striking Miraflores fault that passes nearly through Guatapé. A zone of gouge in this fault several meters thick was penetrated in tunnels of the Nare hydroelectric project between Guatapé and San Rafael (ALVAREZ A., R. oral commun., 1967).

Here and there, outcrops in the batholith are crossed by small faults marked with thin planar or gently curved seams of light green mylonite from a few millimeters to rarely as much as 10 cm thick. Displacements of these small faults are not discernable owing to the rock they cut. Only where they have offset dikes can their displacements be measured (Fig.17). Displacements rarely exceed five meters and are commonly only a few centimeters. The small faults were probably caused by mecanical adjustment during the cooling of the batholith and are regionally unimportant structural features.

The east-central part of the batholith is host to a series of shear zones whose northwest strikes rudely parallel those of the long intrusion faults. The largest, the Cristales shear zone, is 25 km long and follows the projected northwest extension of an intrusion fault west of Caracolí. It is the only shear zone spatially related to an intrusion fault. Other shear zones more than 10 km long are the Sofía shear zone just southwest of the Cristales, and an unnamed shear zone south of Yalí. The shear zones are considered apart from the faults because of their unique characteristics. They are confined exclusively to the batholith, the thickness of sheared rock in them is very great, in places as much as 750 meters, and they have very weak topographic expression.

Most of the shear zones are poorly exposed. They have been recognized largely from loose residual cobles or boulders or mylonite, or from exposures in weathered rock. Only the Cristales shear zone is well exposed in fresh rock in cuts along the road to the sttlement of Cristales. Moderately sheared rock is strongly foliated, dark gray, fine grained, and resembles biotite schist. In the section it is patently cataclastic. More intensely sheared rock is relatively massive, nearly black with a dull luster, and very fine grained. Superficially it resembles serpentinite, but thin sections show it to be composed of esentially the same minerals, though very finely comminuted, as the less sheared rock.

The origin of the shear zones is somewhat obscure. Their confinement to the batholith and great thickness implies that they were zones of repeated and prolonged movement which first may have become active in the late magmatic stage of the batholith.

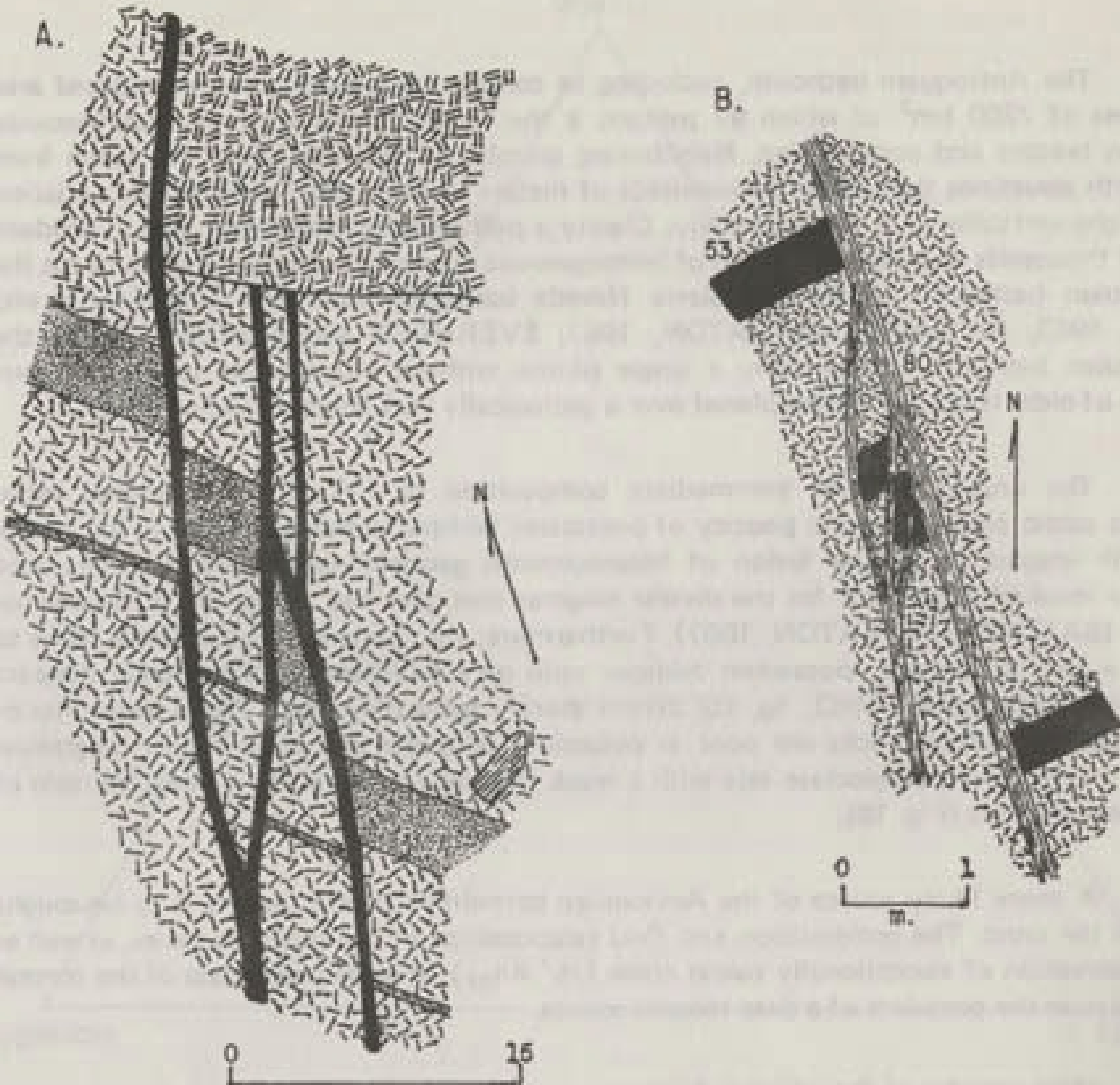

FIGURE 17. Small faults in the Antioquian batholith and a consaguinous stock. Related to the cooling (?). A: Symbols, single line shading, quartz diorite, double line shading, alaskite; stippled, felsite; dark lines, mylonite. The alaskite cuts some of the faults but in turn is cut by another one. The inclusion in the lower section of the sketch is feldspathic gneiss. Quebrada Farallones, elevation 1350 m. B: Symbols; single line shading, quartz diorite; black, dacite - Río Nus, 2 km upstream from Caracolí. Field sketches by T. Feininger.

10. ORIGIN

The junior author first ascribed a magmatic origin to the Antioquian batholith (BOTERO, A., 1963, p. 81-82). In three later papers, Radelli (1965a, b, c) championed an origin by metasomatic replacement in situ of pre-existing rocks. The following observations, gleaned largely from earlier pages of our report, leave little doubt but that the batholith must have formed from the intrusion and crystallization of initially hot, uniform magma: sharp and discordant contacts (Fig. 12); rotated inclusions of host rocks (Figs. 14-15); discordant dikes of batholith rock with sharp contacts in host rock, and desilication of dikes where in calcareous rocks (Table 9); uniformity of the dominant normal facies (Table 3); hypidiomorphic texture especially of the normal facies, with such typically igneous petrographic details as interstitial potassium feldspar (Fig.6), zoned plagioclase, and clinopyroxene cores in hornblende (Fig. 8); and enclosure of the batholith in a high-temperature thermal aureole characterized by wollastonite, sillimanite, cordierite and spinel. The sharp and discordant contacts of the batholith and the absence of internal foliation are characteristics shared by plutons intruded into the epizone as defined by Buddington (1959, p. 677-679).

10.1. PETROGENESIS

The Antioquian batholith, excluding its consaguinous stocks, has an exposed area in excess of 7200 km^2 of which 97 percent is the normal facies with its monotonously uniform texture and composition. Neighboring samples of this rock have been taken from sites with elevations that differ by hundreds of meters to more than a kilometer. Variation is as slight vertically as it is horizontally. Clearly a petrogenetic mechanism able to produce tens of thousands of cubic kilometers of homogeneous magma is required to account fot the Antioquian batholith. Unlike the Sierra Nevada batholith, California (BATEMAN and others, 1963; BATEMAN and EATON, 1967; EVERNDEN and KISTLER, 1970) the Antioquian batholith is essentially a single pluton without a composite nature, without screens of older rocks, an was emplaced over a geologically very short period of time.

The uniformity and intermediate composition of the dominant normal facies with its calcic plagioclase and paucity of potassium feldspar argue against an origin of the batholith magma by partial fusion of heterogeneous geosynclinal sediments as has been recently invoked to account for the diverse magmas that gave rise to the Sierra Nevada batholith (BATEMAN and EATON, 1967). Furthermore, the tendency of the Sierra rocks to follow a constant quartz: potassium feldspar ratio on a feldspar-quartz triangular diagram (BATEMAN and others, 1963, fig. 15) differs sharply from the normal facies of the Antioquian batholith whose rocks are poor in potassium feldespar and on a similar diagraman cluster on the quartz-plagioclase side with a weak tendency to maintain a constant ratio of those two minerals (Fig. 18).

A more likely source of the Antioquian batholith's parent magma is to be sought beneath the crust. The composition and field relationships of the gabbroic facies, as well as the preservation of exceptionally calcio cores ($\sim An_{85}$) in some plagioclase of the normal facies sustain the postulate of a deep magma source.

Most samples of the gabbroic facies are considerably altered rocks rich in pale green, fibrous, secondary amphibole and chlorite after pyroxene or hornblende, "iddingsite" and talc after olivine, and saussuritized plagioclase. Outward these altered rocks grade progressively into fresher rocks: hornblende gabbro, hornblende diorite, and finally the normal facies of the batholith, chiefly quartz diorite. In the largest body of the gabbroic facies, however, that between San José and Cristales, gabbroic rocks surround a core of ultramaphic rock, chiefly pyroxenite (Table 6 col. 1). Our interpretation is that all bodies of the gabbroic facies were initially inclusions of ultramafic rock and that these were swept up and carried along by the ascending batholith magma at the time of intrusion. The ultramafic rocks are considered samples of the environment in which the batholith magma was generated, a subcrustal ultramafic environment. Out of equilibrium with their new surroundings, the ultramafic inclusions reacted with the enclosing magma of quartz diorite and granodiorite composition to form a suite of gabroic rocks enriched in secondary minerals. These altered rocks grade outward into less mafic rocks, hornblende gabbro and hornblende diorite, that were stable under the conditions prevalent in the crystallizing batholith. Only the inclusion now found between San José and Cristales was large enough to prevent the destruction of all ultramafic rock by reaction and a small unaltered core remains preserved. Perhaps the gabarros, the small mafic clots so characteristic of the normal facies (Fig.10), represent small inclusions of ultramafic rock where reaction has gone to completion. Potassium feldspar, a major constituent of many gabarros occurs as interstitial fill which postdates the other minerals.

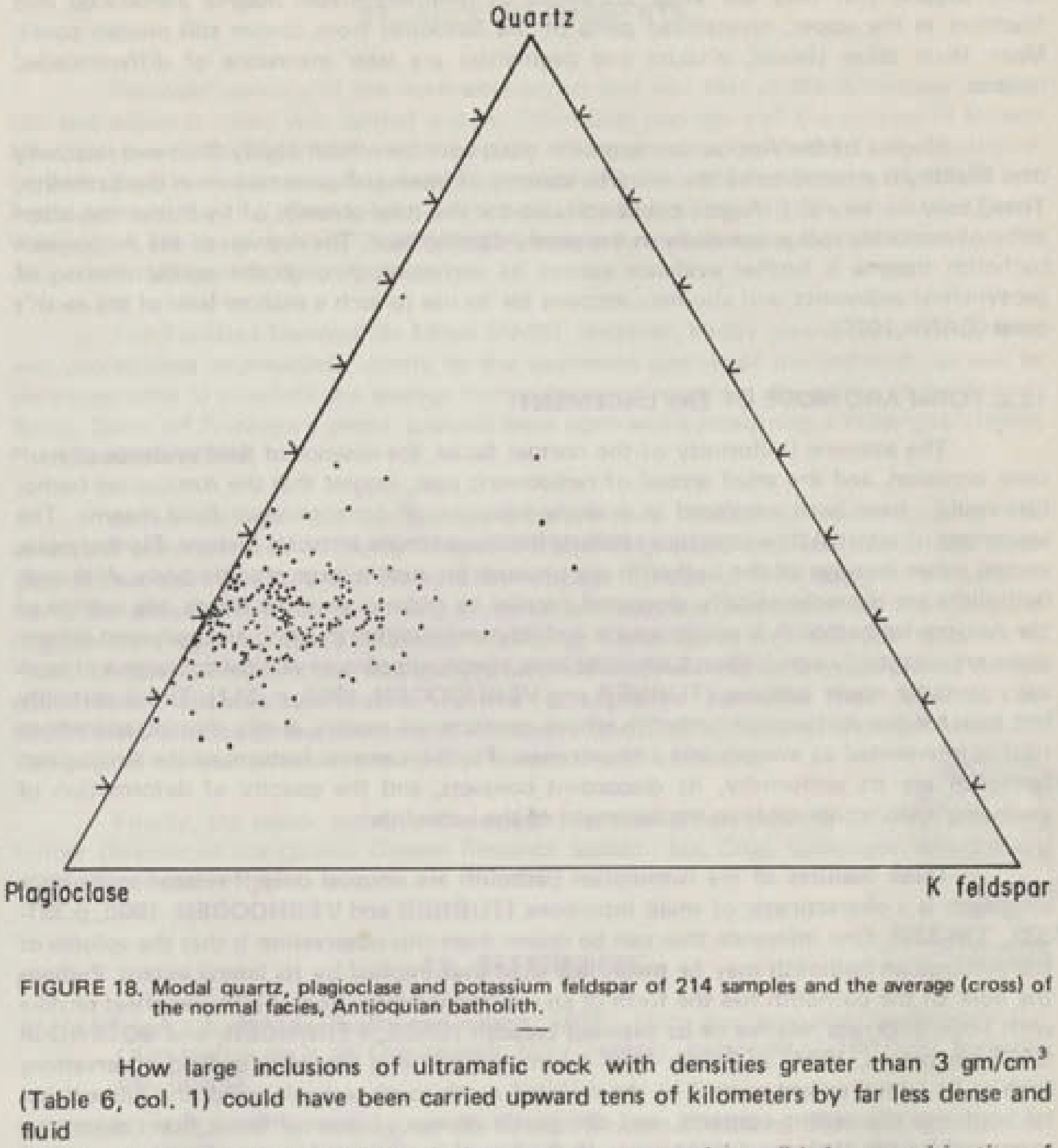

FIGURE 18. Modal quartz, plagioclase and potassium feldspar of 214 samples and the average (cross) of the normal facies, Antioquian batholith.

How large inclusions of ultramafic rock with densities greater than 3 gm/cm³ (Table 6, col. 1) could have been carried upward tens of kilometers by far less dense and fluid magma is uncertain. One possibility is that transport was made possible by a combination of two factors: relatively swiftly moving magma, and irregular shapes of the inclusions themselves.

Uncertainty in the nature of the contact of the felsic facies greatly inhibits understanding its origin. Both its general petrographic characteristics and radiometric age, however, argue that it is intimately a part of the Antioquian batholith rather than a later, unrelated intrusion. Most likely it represents magma produced by differentiation late in the crystallization history of the batholith that was reintruded into already consolidated rock of the normal facies. The somewhat younger radiometric age of the felsic facies supports this contention.

The thin, fine-grained, intermediate dikes have compositions closely akin to that of the normal facies that they so abundantly cut. This observation and their mode of occurrence suggest that they are small intrusions of undifferentiated magma introduced into fractures in the upper, crystallized parts of the batholith from deeper still molten zones. More felsic dikes (felsite, alaskite and pegmatite) are later intrusions of differentiaded magma.

Magma of the Antioquian batholith must have been both highly fluid and relatively dry. Fluidity is attested to by the extreme scarcity of internal flow structure in the batholith. Then, only a very dry magma could account for the total absence of hydrothermal alteration of enclosing rocks, especially in the gently-dipping roof. The dryness of the Antioquian batholith magma is further evidence against its derivation through the partial melting of geosynclinal sediments, and also may account for its rise to such a shallow level of the earth's crust (CANN,1970).

10.2. FORM AND MODE OF EMPLACEMENT

The extreme uniformity of the normal facies, the absence of field evidence of multiple intrusion, and the small spread of radiometric ages, suggest that the Antioquian batholith could have been emplaced as a single intrusion of homogeneous fluid magma. The sparseness of internal flow structure similarly implies a simple intrusive history. Furthermore, several other features of the batholith are unusual for such a large granitic body. Although batholiths are characteristically elongated parallel to regional tectonic trends, the outline of the Antioquian batholith is nearly square and its maximum north-south and east-west dimensions are essentially equal. Most batholiths have steeply-dipping or vertical contacts and typically irregular upper surfaces (TURNER and VERHOOGEN, 1960, p. 311). This is certainly not true for the Antioquian batholith whose contacts are mostly gently dipping and whose roof is interpreted as smooth and subhorizontal. Further unusual features of the Antioquian batholith are its uniformity, its discordant contacts, and the paucity of deformation of enclosing rocks attributable to emplacement of the batholith.

These features of the Antioquian batholith are unusual only if related to its huge size; each is a charactiristic of small intrusions (TURNER and VERHOOGEN, 1960, p.331-332, 338-339). One inference that can be drawn from this observation is that the volume of the Antioquian batholith may be much less than that implied by its lateral extent. Perhaps the bulk of the batholith has the form of an enormous subhorizontal intrusive sheet or dike with little thickness relative to its exposed breadth (CASE, FEININGER, and BOTERO in CASE an others, 1971, p. 2696). Such a form would be in accord with field observations such as its lateral extent normal to the regional north-south tectonic trend, the subhorizontal roof and discordant contacts, and the gentle plunge of internal linear flow structures expressed by the long axes of gabarros. If the lateral intrusion of magma lifted the roof of the batholith as a more or less integral unit broken only by sporadic intrusion faults, the virtual absence of other deformation in host rocks attributable to emplacement can be explained. Steep contacts are restricted to an area south of San Luis, the only place where the batholith magma invaded incompetent rocks.

Sheetlike intrusions with forms analoguos to that postulated for the Antioquian batholith have been recognized elsewhere. The Curecanti Quartz Monzonite, Colorado, forms a horizontal pluton wholly discordant to igneous and metamorphic host rocks and tapers to feather edges (HANSEN, 1964, p. D6 - D10). A vertical feeder is postulated (HANSEN, 1964, Fig. 2). Crystalline basement rocks in Victoria Land, Antarctica, are host to an enormous subhorizontal sheet of diabase at least 40 by 48 km (HAMILTON, 1965, p.17 - 20). Floor and roof, both exposed in mountainsides (HAMILTON, 1965, Fig. 16 - 17) are everywhere discordant.

11. ACKNOWLEDGMENTS

Geologic mapping of the northwest corner and east half of the Antioquian batholith and adjacent rocks was carried out by Colombian geologists of the Inventario Minero Nacional (now INGEOMINAS) supervised by Feininger, then with the U. S. Geological Survey. The Inventario was a joint program of the Colombian Ministry of Mines and Petroleum and the U. S. Geological Survey, partly financed by USAID, Department of State, Washington. We are grateful to INGEOMINAS and its former Director, Andrés Jimeno V. for cooperation and permission to publish.

The Facultad Nacional de Minas (FNM), Medellín, kindly gave us access to samples and unpublished information, chiefly on the southwest quarter of the batholith, as well as computer time to calculate the average composition and standard deviations of the normal facies. Some of Feininger's modal analysis were done while occupying a Fulbright Visiting Professorship at FNM.

About half the thin sections used by us were provised by the Inventario. The remainder were prepared by Mario Tabares, FNM. The geologic map and its intricate topographic base were skillfully drafted by Lino Arbelaez Z., also of FNM. Many of the calculations, the determination of specific gravities of samples, and preparation of the triangular diagram were done by Darío Arbelárez and Jorge Campuzano, then last-year students at FNM. Cristalería Peldar, Ltda., Medellín, generously made secretarial help and a field vehicle with driver available to Botero. Further cartographic assistance was provided by INGEOMINAS through the courtesy of Humberto González I., Regional Director, Medellín. The original manuscript was typed by Sra. Helena Hoyos de Botero.

Finally, the senior author owes a particular debt of gratitude to Dr. Peter Kramer, former Director of the Charles Darwin Research Station, Sta. Cruz, Galápagos, where most of this paper was written.

12. REFERENCES

ÁLVAREZ A., J., HALL, R. B. and others, 1970, Mapa geológico del cuadrángulo H-8 (Yarumal) y parte del cuadrángulo H-7 (Ituango), Antioquia [1:100,000]: Bogotá, Ingeominas.

BARRERO, L. D., 1979, Geology of the Central Western Cordillera, west of Buga and Rolandillo, Colombia: Bogotá, Pub. Geol. Esp. del Ingeominas no. 4, 75p.

BATEMAN, P. C. and others, 1963, The Sierra Nevada batholith: a systhesis of recent work across the central part: U. S. Geol. Survey Prof. Paper 414-D, 46p.

BATEMAN, P. C. and EATON, J. P., 1967, Sierra Nevada batholith: Science, v. 158, no. 807, p. 1407-1417.

BOTERO A., G., 1940, Sobre el Ordoviciano de Antioquia: Proc. 8th Pan-American Scientific Congress, v. 4, p. 19-25.

----------, 1941, Formaciones geológicas de Antioquia: Medellín, Minería, no. 111, p. 9080-9085.

----------, 1942, Contribución al conocimiento de la petrografía del batolito Antioqueno: Medellín, Minería, no. 115-117, p. 1318-1330.

----------, 1963, Contribución al conocimiento de la geología de la zona central de Antioquia: Medellín, Anales de la Facultad de Minas, no. 57,

101p.

BOUSSINGAULT, J. B., 1825, Sur l'existence d'iode dans l'eau de une saline de la Province d'Antioquia: Paris, Ann. de Chimie et Physique, v. 30, p. 91-96.

BRANNER, J.C., 1896, Decomposition of rocks in Brazil: Geol. Soc. America Bull., v. 7, p. 255-314.

BUDDINGTON, A. F., 1959, Granite emplacement with special reference to North America: Geol. Soc. America Bull., v. 70, p. 671-747.

CAMPBELL, C. J. and BURGL, H., 1965, Section through the Eastern Cordillera of Colombia, South America: Geol. Soc. America Bull., v. 76, p. 567-590.

CANN, J. R., 1970, Upward movement of granitic magma: Geol. Mag, v. 107, p. 335-340.

CASE, J. R. and others, 1971, Tectonic investigations in western Colombia and eastern Panama: Geol. Soc. America Bull., v. 82, p. 2685-2712.

COBBING, E. J. and PITCHER, W. S., 1972, The coastal batholith of central Peru: Geol. Soc. London Jour., v. 128, p. 221-460.

DEER, W. A., HOWIE, R. A. and ZUSSMAN, J., 1963, Rock-forming minerals, v. 2, Chain silicates: New York, John Wiley, 379p.

EMPRESAS PUBLICAS DE MEDELLIN, 1957, Represa de Troneras, diseno preli-minar: Medellín, Integral Ltd., 198p.

----------, 1971, Desarrollo hidroeléctrico de los ríos Nare, Guatapé y Samaná: Medellín, Integral Ltd., 107p.

EVERNDEN, J. F., and KISTLER, R. W., 1970, Chronology of emplacement of Meso-zoic batholith complexes in California and western Nevada: U. S. Geol. Survey Prof. Paper 623, 42p.

FEININGER, T., 1969, Pseudokarst on quartz diorite, Colombia: Zeitschrift für Geo-morphologie, v. 13, p. 287-296.

----------, 1970, The Palestina fault, Colombia: Geol. Soc. America Bull., v. 81, p. 1201-1216.

----------, 1971, Chemical weathering and glacial erosion of crystalline rocks and the origin of till: U. S. Geol. Survey Prof. Paper 750-C, p. 65-81.

----------, 1972, Geología de parte de los departaments de Antioquia y Caldas (sub-zona IIB): Bogotá, Ingeominas.

FUJIYOSHI, A., 1976, Metamorphic and igneous rocks from the Medellín-Yarumal and Santa Marta areas, Colombia, and their Rb/Sr ages: Jour. Geol. Soc. Japan, v. 82, p. 559-563.

GROSSE, E., 1926, Estudio geológico del Terciario Carbonífero de Antioquia: Berlin, Dietrich Reimer, 361p.

HAMILTON, W., 1965, Diabase sheets of the Taylor Glacier region, Victoria Land, Antarctica: U. S. Geol. Survey Prof. Paper 456-B, 71p.

HANSEN, W. R., 1964, Curecanti pluton, an unusual intrusive body in the Black Canyon of the Gunnison, Colorado: U. S. Geol. Survey Bull. 1181-D, 15p.

INVENTARIO MINERO NACIONAL, 1965, Mapa geológico de la plancha I-8 [1:200,000]: Bogotá, Ingeominas.

IRVING, E. M., 1971, La evolución estructural de los Andes más septentrionales de Colombia: Bogotá, Ingeominas, Bol. Geol. v. 19, no. 2, 90p. [See also: IRVING, E. M., 1975, Structural evolution of the northernmost Andes, Colombia: U. S. Geol. Survey Prof. Paper 846, 47p.].

KISTLER, R. W., EVERNDEN, J. F. and SHAW, H. R., 1971, Sierra Nevada plutonic cycle: Part I, Origin of composite granitic batholiths: Geol. Soc. America Bull., v. 82, p. 853-868.

LEAKE, B. E., 1978, Nomenclature of amphiboles: Min. Mag., v. 42, p. 533-563.

McLAUGHLIN, D. H., Jr., 1972, Geology and mineral resources of the Zipaquirá area (zone iv), Cordillera Oriental, Colombia: U. S. Geol. Survey Open-File Report, 332p.

MYERS, J. S., 1975, Cauldron subsidence and fluidization: Mechanisms of intrusion of the coastal batholith of Peru into its own volcanic ejecta: Geol. Soc. America Bull., v. 86, p. 1209-1220

NELSON, H. W., 1957, Contribution to the geology of the Central and Western Cor-dillera of Colombia in the sector between Ibagué and Cali: Leidse Geol. Med., deel 2, p. 1-76.

O'CONNOR, J. T., 1965, A classification for quartz-rich igneous rocks based on feldspar ratios: U. S. Geol. Survey Prof. Paper 525-B, p. 79-84.

OSPINA, T., 1911, Resena geológica de Antioquia: Medellín, Imprenta La Organización, 128p.

PÉREZ A., G., 1967, Determinación de edad absoluta de algunas rocas de Antioquia por métodos radiactivos: Medellín, Dyna, no. 84, p. 27-31.

POSADA, J. de la C., 1936, Bosquejo geológico de Antioquia: Medellín, Anales de la Escuela Nacional de Minas, no. 38, 50p.

RADELLI, L., 1962, Introducción al estudio de la petrografía del macizo de Garzón: Bogotá, Geología Colombiana, no. 3, p. 17-46.

----------, 1965a, Contribution à la géologie de l'occidente Andin Colombien dans les Départements de Caldas et Antioquia: Travaux de Laboratoire de Géologie de la Faculté des Sciences de Grenoble, v. 41, p. 187-208.

----------, 1965b, Note préliminaire sur la géologie et la genèse des granites des Andes: Travaux du Laboratoire de Géologie de la Faculté des Sciences de Grenoble, v. 41, p. 209-218.

----------, 1965c, Metallogenic belts and « igneous » rocks of [the] Colombian Andes: Travaux du Laboratoire de Géologie de la Faculté des Sciences de Grenoble, v. 41, p. 219-228.

RENZONI, G., 1965, Geología del cuadrángulo L-11,Villavicencio: Bogotá, Ingeominas.

ROSS, D. C., 1969, Descriptive petrography of three large granitic bodies in the Inyo Mountains, California: U. S. Geol. Survey Prof. Paper 601, 47p.

RUIZ, C., AUGUIRRE, L., CORVALAN, J., ROSE, H. J., Jr., SEGERSTROM, K. and STERN, T.W., 1961, Ages of batholithic intrusions of northern and central Chile: Geol. Soc. America Bull., v. 72, p. 1551-1559.

SCHEIBE, R. o E. ?, 1933..........

STIBANE, F. R., 1968, Zur Geologie von Colombien, Südamerika: das Quetame- und Garzón-Massiv: Geotektonische Forsch., no. 30, 84p.

TAUBENECK, W. H., 1967, Petrology of Cornucopia Tonalite unit, Cornucopia stock, Wallowa Mountains, northeastern Oregon: Geol. Soc. America Spec. Paper 91, 56p.

TSCHANZ, C. M., JIMENO V., A. and CRUZ B., J., 1969, Mapa geológico de re-conocimiento de la Sierra Nevada de Santa Marta, Colombia: Bogotá, Ingeominas. [See also: TSCHANZ, C. M., MARVIN, R. F., CRUZ B., J., MEHNERT, H. H. and CEBULA, G. T., 1974, Geologic evolution of the Sierra Nevada de Santa Marta: Geol. Soc. America Bull., v. 85, p. 273-284].

TURNER, F. J. and VERHOOGEN, J., 1960, Igneous and metamorphic petrology: New York, McGraw-Hill, 694p.

VAN HOUTEN, F. B. and TRAVIS, R. B., 1968, Cenozoic deposits, upper Magdalena valley, Colombia: Am. Assoc. Petrol. Geol. Bull., v. 52, p. 675-702.

WARD, D. E., GOLDSMITH, R., CRUZ B., J. and others, 1069, Mapas geológicos de los cuadrángulos H-12, H-13 y partes de los cuadrángulos I-12 y I-13: Bogotá, Ingeominas.

WILHELMY, H., 1958, Klimamorphologie des Massengesteine: Braunschweig, Georg Westernamm Verlag, 283p.

WRUCKE, C. T., 1965, Prehnite and hydrogarnet(?) in Precambrian rocks near Boulder, Colorado: U. S. Geol. Survey Prof. Paper 525-D, p. 55-58.

FIG. 3a - GEOLOGIC MAP OF THE ANTIOQUIAN BATHOLITH

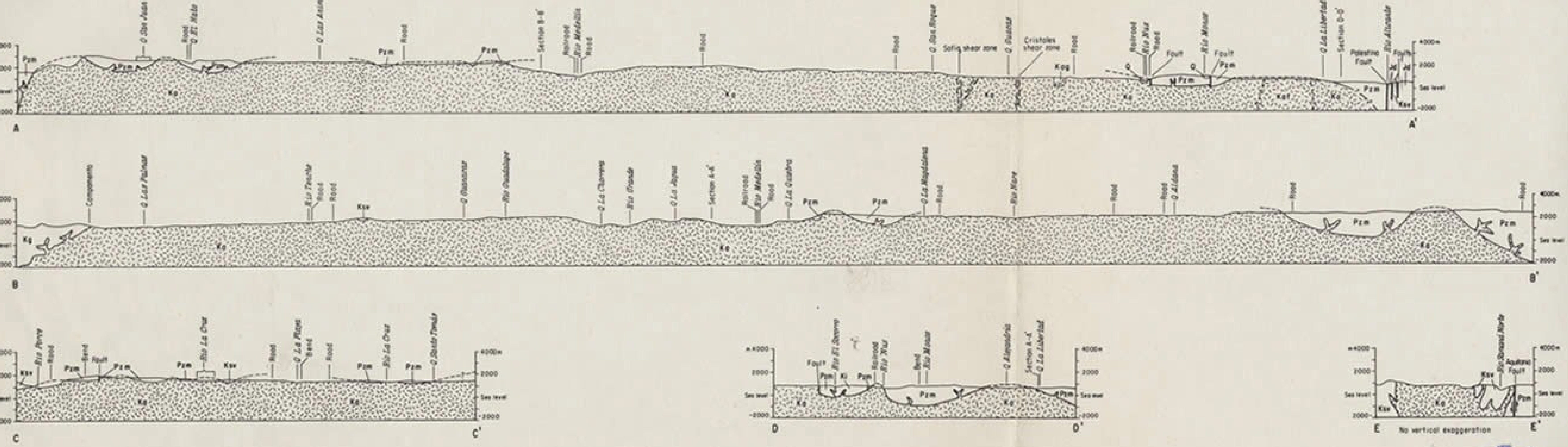

FIG. 3b - GEOLOGICAL SECTIONS OF THE ANTIOQUIAN BATHOLITH